Neutrophils induce effective antibody responses to the pneumococcal conjugate vaccine by inhibiting regulatory T cells

Essi YI Tchalla[1], Anagha Betadpur[1], Andrew Y Khalil[1], Elena Lopez[1], Manmeet Bhalla[1], Musea Chang[1], Elizabeth A. Wohlfert[1] and Elsa N. Bou Ghanem[1,2]*

[1]Author affiliations: Department of Microbiology and Immunology, University at Buffalo School of Medicine, Buffalo, NY 14203, USA

[2]Lead contact

*Correspondence: Elsa N. Bou Ghanem, 955 Main Street, Buffalo, NY, 14203. Telephone: 716-829-2422. Email: elsaboug@buffalo.edu

Running title: PMNs promote vaccination protection by inhibiting Tregs

SUMMARY

Neutrophils are required for production of protective antibodies in response to the pneumococcal conjugate vaccine (PCV), however, the mechanisms behind that are not known. Here, in exploring mechanisms, we found that depletion of neutrophils at the time of vaccination in female mice led to increased regulatory T cells (Tregs) in the spleen that was accompanied by a dysregulated cytokine environment. Following vaccination, neutrophils homed into secondary lymphoid organs where they increased expression of T cell engaging/inhibiting markers. Depletion of Tregs in neutrophil deficient mice restored antibody function against pneumococcal infection. Importantly, PCV vaccination of human female participants altered neutrophil phenotype and *in vitro* coculture of donor neutrophils with PBMCs at one week following vaccination resulted in lower percentage and proliferation of $FOXP3^{+}$ T cells, showing the clinical relevance of this phenotype. This work reveals a new mechanism by which neutrophils ensure protective antibody responses to vaccination by suppressing Tregs.

KEYWORDS

Neutrophils- Pneumococcal conjugate vaccine- *Streptococcus pneumoniae*

53 **INTRODUCTION**

54 Neutrophils or polymorphonuclear cells (PMNs) are innate immune cells that are
55 indispensable for the clearance of many infections and that have been traditionally studied as
56 anti-microbial effector cells (Simmons et al., 2021). However, in the past decade, PMNs have
57 become increasingly appreciated for their ability to orchestrate adaptive immune responses (Bert
58 et al., 2023; Mantovani et al., 2011). In fact, they can affect B and T cells directly or via control of
59 antigen presenting cells such as dendritic cells and macrophages (Leliefeld et al., 2015; Li et al.,
60 2019; Shafqat et al., 2023). They can engage and stimulate T cells in response to antigens via
61 expression of MHC-II, CD80, CD86 and/or CD11c (Abi Abdallah et al., 2011; Culshaw et al., 2008;
62 Matsushima et al., 2013; Vono et al., 2017) or inhibit T cells via production of IL-10, reactive
63 oxygen species, arginase or by expressing PD-L1 (de Kleijn et al., 2013; Kasten et al., 2010;
64 Pillay et al., 2012; Schmielau and Finn, 2001). The ectonucleotidases CD73 and CD39 have been
65 associated with T cell inhibition via adenosine production and are also expressed on PMNs (Allard
66 et al., 2017; Jiang et al., 2023). PMNs can also suppress B cell responses to protein antigens
67 (Bird et al., 2017; Jee et al., 2015; Kamenyeva et al., 2015) or activate B cell responses to
68 bacterial carbohydrates through secretion of B cell activating factor (BAFF), A proliferation-
69 inducing ligand (APRIL), IL-21 or Pentraxin 3 (Chorny et al., 2016; Puga et al., 2011).

70 While most of the work examining PMN interaction with adaptive immune cells have used
71 model antigens, a few studies have recently focused on the role of PMNs in vaccine responses
72 (Musich et al., 2018). In an adenovirus-SIV vaccination model of Rhesus macaques, PMNs were
73 found to migrate to the vaccine draining lymph nodes (vLNs) and acquire a B cell help phenotype
74 as indicated by expression of BAFF, IL-21 and TNFα among others (Musich et al., 2018). PMNs
75 were found to be required for effective immune responses to both tuberculosis and leishmaniasis
76 live-attenuated vaccine models (Bhattacharya et al., 2020; Trentini et al., 2016). In the context of
77 a clinically relevant vaccine, we showed that PMNs are required at the time of vaccination for
78 induction of protective antibody responses to the licensed pneumococcal conjugate vaccine

79 (PCV) Prevnar (Tchalla et al., 2020). In fact, depleting PMNs at the time of PCV vaccination led
80 to a defect in antibody isotype switching to IgG2c and IgG3, a decline in antibody function, and
81 decreased ability of the mice to control and survive a subsequent pneumococcal infection (Tchalla
82 et al., 2020). However, the mechanisms by which PMNs control antibody responses to PCV
83 remain unclear. This is of high clinical relevance as PCV protects against infections caused by
84 the bacteria *Streptococcus pneumoniae* (pneumococcus), which remain a leading cause of
85 community acquired pneumonia globally, particularly in vulnerable populations such as older
86 adults (CDC, 2022). Understanding the mechanisms behind vaccine efficacy can lead to design
87 of better vaccines.

88 Conjugate vaccines such as PCV induce T follicular helper cells (Tfh) that aid the
89 production of antibodies by B cells (Rappuoli, 2018; Vinuesa et al., 2016). In fact, PCV vaccination
90 in humans induced the formation of Tfhs, which was linked to enhanced antibody responses
91 (Sterrett et al., 2020). Following vaccination with a conjugate vaccine, germinal centers (GC) form
92 and mature within secondary lymphoid organs such as the lymph nodes (LNs) and spleen (De
93 Silva and Klein, 2015; Pollard et al., 2009). Inside GCs, polysaccharide-specific B cells acquire
94 conjugate antigens from the surface of follicular dendritic cells and process them intracellularly
95 for presentation to Tfhs (De Silva and Klein, 2015; Pollard et al., 2009; Rappuoli et al., 2019a).
96 Interaction between the Tfhs and GC B cells triggers B cell differentiation into antibody secreting
97 cells and enhances antibody production, class switching and affinity maturation (Murphy et al.,
98 2017; Rappuoli et al., 2019b). These antibodies are required for efficient host protection against
99 infections as they facilitate binding, uptake, and killing of bacteria by phagocytes (Forthal, 2014;
100 Vidarsson et al., 2014). Antibody responses by B cells are also highly influenced by cytokines,
101 which are secreted by Tfhs as well as other T cell subsets (Dong, 2021; Vazquez et al., 2015;
102 Vinuesa et al., 2016).

103 A subset of T cells known to control immune responses are regulatory T cells (Tregs).
104 Tregs have suppressive capacity and play an essential role in homeostasis and immune tolerance

105 (Shevyrev and Tereshchenko, 2019). In the context of vaccination, Tregs have been shown to
106 limit protective immune responses (Bayry, 2014; Moore et al., 2005; Ndure and Flanagan, 2014;
107 Pere et al., 2012; Stepkowski et al., 2024; Weingartner and Golding, 2017). In multiple HIV and
108 cancer models of vaccination, Tregs were shown to dampen both cellular and humoral immune
109 responses, leading to viral replication or tumor progression (Brezar et al., 2015; Togashi et al.,
110 2019). In a pneumococcal polysaccharides model of vaccination, blocking the Treg effector
111 molecule CTLA-4 enhanced antibody and cytokine responses to the polysaccharides (Boudewijns
112 et al., 2005). In humans, higher Tregs in the PBMC of older adults were associated with lower
113 $CD4^+$ T cell responses to immunogenic pneumococcal proteins (He et al., 2021). A subset of
114 Tregs that gain access to B cell follicles are termed T follicular regulatory cells or Tfr (Lu and Craft,
115 2021; Maceiras et al., 2017). Tfrs display phenotypic markers of T follicular helper cells (Tfhs), in
116 addition to their expression of FOPX3 (Maceiras et al., 2017; Qi et al., 2023). They play a role in
117 humoral responses to antigens that is context dependent and have been shown to inhibit B cell
118 responses and accelerate GC contraction (Jacobsen et al., 2021; Sage et al., 2016; Xie et al.,
119 2020). Several studies have looked at the relationship between Tregs and PMNs in models of
120 inflammation and disease and found that Tregs modulate PMN recruitment to the site of
121 inflammation (Himmel et al., 2011; Lewkowicz et al., 2013; Richards et al., 2010). PMNs in turn
122 also promote Treg recruitment in autoimmune and cancer models, and their depletion leads to a
123 decrease in Tregs (Gao et al., 2015; Mishalian et al., 2014; Nadkarni et al., 2016; Perobelli et al.,
124 2016). The interaction of PMNs and Tregs during vaccine responses (including PCV) has not
125 been studied.

126 In this study, we tested the effect of PMNs on adaptive immune responses to PCV using
127 a preclinical murine model of vaccination as well as by examining responses in vaccinated human
128 participants. We found that following vaccination, PMNs acquire a T cell engaging and
129 suppressing phenotype and suppress Tregs, which is required for the production of protective
130 antibodies. This study reveals a new mechanism by which PMNs shape vaccine responses

131 through the control of Tregs and provides novel targets for the design of more effective vaccines
132 against bacterial infections.
133
134 **RESULTS**
135 **PMNs home into secondary lymphoid organs in response to PCV**
136 In prior work, we showed that PMNs are required at the time of PCV administration for the
137 induction of effective antibody response and optimal host protection against pneumococcal
138 disease (Tchalla et al., 2020). There is a well-documented sex-based difference in responses to
139 PCV where females elicit higher antibody responses and vaccine efficacy compared to males
140 (Soneji and Metlay, 2011; Wagenvoort et al., 2017; Wiese et al., 2016) and we recapitulated this
141 in preclinical murine models (Tchalla et al., 2024). Therefore, to understand mechanisms of
142 protection, we focused our studies on female hosts, that mount higher humoral and cellular
143 responses to PCV and are better protected against subsequent pneumococcal infection
144 compared to male hosts (Tchalla et al., 2024).
145 To better understand how PMNs control PCV efficacy, we first asked whether they are
146 recruited to secondary lymphoid organs (spleen and vaccine draining lymph nodes (vLNs)) in
147 response to vaccination. We looked at expression of migration markers CXCR4 and CCR7 on
148 circulating PMNs 24 hours post vaccination as they are involved in PMN trafficking to the lymph
149 nodes via the lymphatic system or high endothelial venules (Fig. S1 & Fig. 1A) (Beauvillain et al.,
150 2011; Hampton et al., 2015). We found that at baseline, a low percentage of circulating PMNs
151 express CXCR4 and CCR7 and upon vaccination, $CCR7^{+}$ PMNs significantly increase (Fig. 1A).
152 This higher percentage of $CCR7^{+}$ PMNs coincided with a decrease in the number of circulating
153 PMNs 18 to 24 hours post vaccination and an influx of PMNs to the spleen and vLNs at those
154 time points respectively (Fig. 1B). Following the peak of PMN influx into the spleen and vLNs,
155 PMN numbers return to baseline by 48 hours post vaccination (Fig. 1B). These findings
156 demonstrate that PMNs are rapidly recruited to secondary lymphoid organs in response to PCV.

157

158 **PMNs do not affect B cell numbers in response to PCV**

159 To start investigating how PMNs induce protective antibodies to PCV, we first examined
160 changes to the B cell compartment. We depleted PMNs at the time of vaccination as presented
161 in Fig S2A and previously described (Tchalla et al., 2020). The efficiency of PMN depletion was
162 assessed over 28 days post vaccination in the spleen (Fig. S2B). We observed >90% PMN
163 depletion at day 7 (Fig. S2B) with a return to steady state numbers in the spleen by day 28 (Fig.
164 S2B) (Tchalla et al., 2020). We then investigated B cell responses post PMN depletion in the
165 spleen on days 7, 14 and 21 post vaccination (Fig. S3A). Upon PMN depletion, there was no
166 change in the percentage and numbers of total B cells ($B220^{+}$) in the spleen compared to isotype
167 treated mice at any of the timepoints investigated (Fig. S4A). Similarly, no effect of PMN depletion
168 was observed on GC B cells ($CD38^{lo}CD96^{+}$) and plasmablasts ($CD138^{+}$) (Fig. S4B & S4C). In
169 prior work, we had observed a defect in isotype switching, opsonic and binding capacities of
170 antibodies in response to PCV in PMN deficient hosts (Tchalla et al., 2020), indicating a possible
171 defect on somatic hypermutation (SHM) and/or class switch recombination (CSR). Therefore, on
172 days 7 post vaccination, we assessed B cell expression of Activation Induced Cytidine Deaminase
173 (AID), an enzyme required for both SHM and CSR (Di Noia and Neuberger, 2007; Stavnezer et
174 al., 2008) (Fig. S3B). For both total and GC B cells, there was an increase in AID expression in
175 mice following vaccination (Fig. S5). However, depleting PMNs had no effect on the percentage
176 of AID^{+} B cells or the expression of AID by B cells (Fig. S5). These findings suggest that PMNs
177 are not directly acting on B cells during vaccination.

178

179 **PMNs do not affect macrophages and dendritic cells in response to PCV**

180 We then looked at the effect of PMNs on other immune cells important for vaccine
181 responses such as antigen presenting cells (APCs) (Abi Abdallah et al., 2011; Morel et al., 2008).
182 For that, we depleted PMNs at the time of vaccination (Fig. S2) and analyzed the percentage of

183 splenic macrophages (F4/80$^+$) and dendritic cells (DC-CD11c$^+$) or their respective expression of
184 antigen presenting molecules MHC-II, CD80 and CD86 on days 7, 14 and 21 post vaccination
185 (Fig. S6). Overall, we found that depletion of PMNs had no effect on the percentages of both
186 macrophages and DCs present in the spleen (Fig. S7). No substantial difference in expression of
187 CD80, CD86 and MHC-II by DCs and macrophages was observed between PMN depleted and
188 PMN sufficient mice (Fig. S7). These findings suggest that PMNs are not directly acting on
189 macrophages or DCs immediately upon vaccination.
190
191 **Absence of PMNs at the time of vaccination alters the cytokine environment in the spleen**
192 The cytokine environment in secondary lymphoid organs controls the quality of antibodies
193 produced (Abbas et al., 1993). Therefore, we next looked more broadly at the overall inflammatory
194 environment in the spleen in the presence or absence of PMNs in vaccinated mice using a
195 cytokine protein array. We found that overall, in the absence of PMNs at the time of vaccination,
196 there was an increase in inflammatory mediators in the splenic milieu compared to when PMNs
197 are present (Fig. S8). This increase in inflammation was seen at day 7 and resolved by day 14
198 through 21 post vaccination (Fig. S8), timepoints that coincide with return of PMNs after depletion
199 (Fig. S2B) (Tchalla et al., 2020). These data show that the absence of PMNs at the time of
200 vaccination leads to an altered inflammatory response in the spleen, suggesting a regulatory role
201 for PMNs during PCV.
202 We had observed a defect in isotype switching to IgG2 and IgG3 antibodies in the absence
203 of PMNs (Tchalla et al., 2020), therefore, we directly tested whether PMNs controlled effective
204 antibody response to PCV through IFNγ, as this cytokine is required for class switching to those
205 isotypes (Karachunski et al., 2000; Murphy et al., 2017). We measured the percentage of IFNγ$^+$
206 PMNs in the spleen 18 hours post vaccination following *ex vivo* stimulation with PMA, heat-killed
207 *S. pneumoniae* or PCV (Fig. S9). We found that more PMNs express IFNγ when stimulated with

208 PMA, however, there was no change in the percentage of IFNγ$^+$ PMNs following vaccination and
209 upon restimulation (Fig. S10A). Similarly, total IFNγ levels in the spleen within the first 28 days of
210 vaccination were comparable between PMN-depleted and PMN-sufficient mice (Fig. S10B).
211 Additionally, when we blocked IFNγ *in vivo* at the time of vaccination using an αIFNγ antibody
212 following the same schedule as for the depletion of PMNs shown in Fig. S2A, there was no effect
213 on bacterial burden in the lung and blood at 24 hours post infection (Fig. S10C) or on host survival
214 (Fig. S10D) compared to the isotype-treated mice. To verify that the blocking antibody was
215 functioning, we measured isotype switching to IgG2 which is controlled by IFNγ (Murphy et al.,
216 2017), and founded that blocking IFNγ led to an increase in IgG1 antibodies and decrease in
217 IgG2b and IgG2c (Fig. S10E). In summary, these data indicate that overall, the control of
218 pneumococcal antibody responses by PMNs is not mediated by IFNγ.
219
220 **PMNs acquire a T cell regulating phenotype upon entry into secondary lymphoid organs**
221 To better understand how PMNs control PCV efficacy, we assessed how they respond to
222 vaccination. PMNs have been shown to acquire different phenotypes depending on entry into
223 organs/tissues and the composition of the tissue microenvironment (Ballesteros et al., 2020; Yang
224 et al., 2019). Therefore, we examined PMN phenotype within the first 24 hours post vaccination
225 when they influx into secondary lymphoid organs (Fig. 1B). As the cytokine responses in the
226 spleen suggested that PMNs play a regulatory role, we looked at the expression of various T cell
227 engaging (MHC-II, CD80, CD86 and CD11c) and suppressing (PDL-1, CD73, CD39 and ARG1)
228 markers on PMNs (Fig. S1B). In all sites investigated, overall, expression of both T cell engaging
229 and suppressing markers on PMNs did not change upon vaccination except for a decrease in PD-
230 L1$^+$ PMNs in the blood and spleen (Fig. S11 & S12). However, there were tissue specific
231 differences regardless of vaccination status (Fig. S11, S12 & 1C). Expression of CD80, CD86,
232 CD11c MHC-II and ARG1 were higher on PMNs in secondary lymphoid organs compared to

233 circulating PMNs in both naïve and vaccinated mice (Fig. S11, S12 & 1C). These data are
234 consistent with the literature showing that entry into tissues instructs PMNs to acquire organ
235 specific phenotypes (Ballesteros et al., 2020; Yang et al., 2019). Additionally, the data suggest
236 that as PMNs influx into secondary lymphoid organs following vaccination (Fig. 1B), they acquire
237 a tissue specific regulatory phenotype. As this PMN population decreases in the blood and enters
238 secondary lymphoid organs (Fig 1B), they may play a role on T cell responses at those sites.
239

240 **PMNs do not affect T helper cell responses to PCV**

241 To test the effect of PMNs on T cell responses, we depleted PMNs at the time of
242 vaccination (Fig S2) and measured the percentages and numbers of T helper 1 (Th1)
243 ($CD4^+TCR\beta^+FOXP3^-Tbet^+$), Th2 ($CD4^+TCR\beta^+FOXP3^-GATA3^+$), Th17 ($CD4^+TCR\beta^+FOXP3^-$
244 $ROR\gamma t^+$) and Tfh ($CD4^+TCR\beta^+CXCR5^+PD1^+$) cells and in the spleen 7-, 14- and 21-days post
245 vaccination (Fig. S13). We found that there was no difference in the percentages or numbers of
246 any of the T cell subsets between vaccinated PMN-depleted and PMN-sufficient mice at any the
247 timepoints investigated in the spleen (Fig. S14). As examining total $CD4^+$ T cells may mask
248 changes within the smaller antigen experienced population, we also looked at antigen
249 experienced cells by gating on $CD49d^+CD11a^+$ T cells (Fig. S13A) (Christiaansen et al., 2017).
250 Similarly, we found no effect of PMN depletion on antigen experienced Th1, Th2, Th17 and Tfhs
251 in the spleen (Fig. S15).

252 As depleting PMNs had no effect on the amount of T helper cells (Fig. S14 & S15), we
253 asked if their ability to produce cytokines was impaired. We examined cytokine responses *ex vivo*
254 using PMA/Ionomycin as positive stimulant for cytokine production. Using flow cytometry, we
255 measured expression of IFNγ, IL-4, IL-17, TGFβ and IL-10 by splenic $CD44^{hi}$ activated $CD4^+$ T
256 cells at day 14 post vaccination (Fig. S16). We used the protein Latency Associated Peptide (LAP)
257 as a proxy for TGFβ production since it acts as a chaperone for TGFβ and their levels correlate

258 (Areström et al., 2012; Liu et al., 2021). The cytokine response was skewed towards production
259 of IFNγ and LAP, both in the presence and absence of PMNs, as the percentage of $CD4^+TCR\beta^+$
260 T cells expressing these cytokines was higher than the other cytokines investigated (Fig. S17).
261 Overall, PMA/Ionomycin stimulation increased LAP, IFNγ and IL-4 expression by $CD44^{hi}$ $CD4^+$ T
262 cells above the no stimulation condition (Fig. S17A-C). However, PMN depletion did not affect
263 expression of any of the cytokines by T cells in comparison to PMN-sufficient mice (Fig. S17).
264
265 **PMNs inhibit Treg expansion in the spleen in response to PCV**
266 We next assessed the effect of PMNs on regulatory T cells (Tregs) ($CD4^+TCR\beta^+FOXP3^+$)
267 and T follicular regulatory cells (Tfrs) ($CD4^+TCR\beta^+CXCR5^+PD1^+FOXP3^+$) following PCV (Fig. 2).
268 We saw an increase in the percentage of Tregs in the spleens of PMN-depleted mice compared
269 to PMN-sufficient mice at day 14 post vaccination (Fig. 2A). In PMN-depleted mice, there was
270 also an increase in the percentage and numbers of Tfrs at day 7 as well as an increase in
271 percentage at day 21 post vaccination (Fig. 2B). When looking at the antigen experienced
272 compartment, there was an increase in Tregs at days 7 and 14 post vaccination in the spleen of
273 PMN-depleted mice compared to PMN-sufficient mice (Fig. 2C) and differences in the Tfrs
274 compartment at days 7 and 21 (Fig. 2D). No differences in Tregs or Tfrs were observed in the
275 lymph nodes (data not shown). These data suggest that PMNs inhibit the expansion of regulatory
276 T cells in the spleen following PCV.
277
278 **PMNs inhibit Treg expansion in response to PCV *in vitro***
279 To directly assess the effect of PMNs on Tregs, we used *in vitro* assays. For that, we
280 performed coculture assays of splenocytes isolated from day 1-vaccinated mice in the presence
281 or absence of PMNs using heat-killed bacteria that contain bacterial polysaccharides or αCD3 as
282 stimulants for 48 hours. PMNs were removed from splenocytes using positive isolation magnetic

283 sorting. Similar to what we observed *in vivo*, in the absence of PMNs, there was an increase in
284 the percentage of Tregs in response to stimulation with heat-killed *S. pneumoniae* (Fig. 3). PMN
285 removal did not alter other T helper cell subsets (Fig. S18). This recapitulates the *in vivo* findings
286 and suggests that PMNs control Tregs response to bacterial polysaccharides.
287
288 **Reducing Tregs in PMN-depleted hosts rescues antibody responses**
289 Next, we tested whether the increase in regulatory T cells is responsible for the defective
290 antibody responses seen in the absence of PMNs at the time of vaccination (Tchalla et al., 2020).
291 To investigate this, we depleted Tregs using an αCD25 antibody (Farkas et al., 2013) either alone
292 or in conjunction with PMN depletion using αLy6G (Fig. S19A). We achieved ~90% depletion of
293 PMNs in the blood and ~40-50% depletion of Tregs in both spleen and blood (Fig. S19B & S19C).
294 Moreover, αCD25 and αLy6G injections had no effect on percentages of Th1, Th2, Th17, Tfhs
295 and B cells in the spleen (Fig. S19D).
296 We then followed antibody levels upon Treg and/or PMN depletion in the blood of mice at
297 weeks 0, 2 & 4 post vaccination. We found an increase in total IgG against pneumococcal
298 polysaccharides in PMN-& Treg-depleted mice compared to PMN-depleted mice at 4 weeks post
299 vaccination (Fig. 4A). We next investigated the ability of antibodies in the sera to bind the surface
300 of the pneumococcus (Fig. S20). In all mouse groups, vaccination significantly increased binding
301 of IgG to the bacteria compared to baseline (Fig. 4B). As previously reported, sera from
302 vaccinated PMN-depleted mice had significantly lower IgG binding compared to sera from
303 vaccinated PMN-sufficient mice (Fig. 4B) (Tchalla et al., 2020). Interestingly, depletion of Tregs
304 in PMN-depleted mice rescued IgG binding in the sera to similar levels to that of PMN-sufficient
305 vaccinated mice, while depletion of Tregs alone did not affect IgG binding in the sera of PMN-
306 sufficient vaccinated mice (Fig. 4B). We also looked at the ability of antibodies in the sera to
307 promote opsonophagocytic killing of the pneumococcus by PMNs isolated from naïve mice. As
308 expected, there was an increase in bacterial killing by PMNs when sera from vaccinated versus

309 naïve mice were used as opsonins (Fig. 4C). Similar to above, depletion of Tregs in PMN-depleted
310 mice rescued the ability of the sera to induce opsonophagocytic bacterial killing to levels similar
311 to PMN-sufficient vaccinated mice, while depletion of Tregs alone did not affect the opsonic
312 capacity of sera from PMN-sufficient vaccinated mice (Fig. 4C).

313 To confirm these findings, we used a different model of Treg depletion for assessment of
314 antibody responses to PCV using diphtheria toxin (DT) mediated depletion (Jin et al., 2017). For
315 that, we used DT injections to deplete Tregs either alone or in conjunction with PMN depletion in
316 DEREG mice (Lahl et al., 2007) (Fig. S21A). We achieved ~25% depletion of Tregs in the spleen
317 (Fig. S21B). Treg depletion in PMN-depleted DEREG mice increased their IgG levels 4 weeks
318 post vaccination compared to vehicle treated PMN-depleted mice (Fig. S21C). The above data
319 suggest that the increase in Tregs seen in PMN-depleted mice contributes to the defective
320 antibody response observed in these mice as reduction of the Tregs rescues the levels and
321 function of the antibodies to similar levels seen in PMN-sufficient vaccinated mice and reduction
322 of Tregs alone in PMN-sufficient vaccinated mice has no effect.

323

324 **Reducing Tregs in PMN-depleted hosts rescues the protective capacity of the sera against**
325 **pneumococcal infection**

326 Finally, we assessed the protectiveness of the sera from PMN- and/or Treg-depleted mice
327 *in vivo* against infection by adoptively transferring sera from each group into naïve mice. Recipient
328 mice were then infected 1hr later with $3x10^5$ CFU of *S. pneumoniae* TIGR4 strain, assessed for
329 blood bacterial burden 48 hours post infection, and monitored for survival. Recipients of sera from
330 vaccinated PMN-sufficient mice were able to control bacterial numbers better than the ones
331 receiving sera from vaccinated PMN-depleted mice with 50% and 87.5% of the mice becoming
332 bacteremic respectively (Fig. 5A). Receiving sera from PMN- & Treg-depleted mice rescued the
333 ability of the recipients to control infection with only 25% of the mice becoming bacteremic (Fig.
334 5A). Additionally, receiving sera from Treg-depleted mice did not affect control of blood bacterial

335 burden (Fig. 5A). Looking at survival, only 10% of recipients of sera from naïve mice survived the
336 infection compared to ~70% of the recipients of sera from vaccinated PMN-sufficient mice (Fig.
337 5B). Receiving sera from PMN-depleted mice resulted in only 30% survival, compared to ~81%
338 survival of mice that received sera from PMN- & Treg-depleted mice (Fig. 5B). The above data
339 suggest that reduction of Tregs in PMN-depleted mice rescues the protectiveness of the sera to
340 levels similar to PMN-sufficient vaccinated mice.
341
342 **Vaccination of human participants alters the phenotype of circulating PMNs**
343 As PMN responses vary significantly across species (Nauseef, 2023), we wanted to test
344 the clinical relevance of these findings. To do so we recruited unvaccinated adult female
345 participants, administered PCV to them, and monitored the phenotype of PMNs in the circulation
346 over time in response to vaccination by examining the expression of T cell engaging and inhibiting
347 markers using flow cytometry (Fig. S22). To test if PMNs respond to PCV and alter their
348 phenotype, we used the OMIQ software to perform opt-SNE analysis to visualize the data, and
349 cluster them using FLOWSOM. We found that PMNs separated into different clusters with varying
350 levels of maturity (based on CD10 expression, Fig. 6A and S23) with cluster 6 being highest
351 followed by 3, 2, 4, 1, 9, 7, 5, and 8 the lowest. Clusters 6 (most mature) was the only cluster that
352 expressed PDL-1 and had high levels of all the other markers, while cluster 8 (least mature), did
353 not express any of the markers we tested (Fig. 6A, 6C and S23). Upon vaccination, we observed
354 a shift in the abundance of circulating clusters where cluster 1, 2 and 6 decreased in abundance,
355 cluster 3, 4 and 5 increased, while cluster 7 and 8 did not change (Fig. 6B). The clusters that
356 decreased from the circulation expressed the highest levels of CD39, ARG1 and HLADR (Fig.
357 6C) and may be homing to the tissues as we observed in mice. When we examined the expression
358 levels of the various markers at week 1 following vaccination, we found that expression of HLADR,
359 CD86, CD39 and PDL-1 increased on all the clusters that expressed them, CD73 either increased
360 or decreased depending on the cluster, while ARG1 decreased (Fig. 6C). Overall, these findings

361 suggest that in response to PCV in humans, the phenotype of circulating PMNs changes, where
362 particular clusters increase expression of T cell engaging and suppressing markers and possibly
363 exit from the circulation into tissues.
364
365 **PMNs from PCV immunized donors inhibit FOXP3$^+$ T cell expansion *in vitro***
366 Finally, we tested whether PMNs from vaccinated participants can suppress FOXP3$^+$
367 CD4$^+$ T cells. For that, at one week post vaccination, a timepoint where we observed phenotypic
368 changes in PMNs in response to vaccination (Fig. 6), we performed an *in vitro* assay where
369 PBMCs from each participant were cocultured with or without PMNs (from the same donor) and
370 stimulated with PCV for 48 hours and T cells assessed (Fig. S24). Similar to what we found in
371 the preclinical model, the presence of PMNs resulted in reduction of FOXP3$^+$ T cells. Addition of
372 PMNs to PBMC cultures lead to a decrease in the percentages of total and antigen experienced
373 FOXP3$^+$ T cells in 67% of participants (Fig. 7A). We also observed a decrease in Ki67$^+$ antigen
374 experienced FOXP3$^+$ T cells in the presence of PMNs in 100% of the participants (Fig. 7B),
375 suggesting that PMNs were suppressing proliferation. These data suggest that PMNs inhibit
376 FOXP3$^+$ T cell responses in humans following PCV administration.
377
378 **DISCUSSION**
379 There are a growing number of studies investigating the effect of neutrophils on adaptive
380 immune responses with a few of them focusing on vaccine responses (Bhattacharya et al., 2020;
381 Musich et al., 2018; Trentini et al., 2016). In this study, we report a new mechanism by which
382 PMNs control antibody responses to the clinically relevant PCV by controlling Treg numbers. In
383 fact, when neutrophils were depleted at the time of PCV vaccination, there was an expansion in
384 the number of Tregs that resulted in a defect in protective antibody responses (Tchalla et al.,
385 2020). Reduction of Tregs in PMN-deficient vaccinated mice boosted antibody number, function,
386 and protective efficacy in the sera. This work demonstrates that PMNs drive production of

387 functional antibodies against pneumococci in response to PCV by limiting the expansion of
388 immune suppressive Tregs.

389 While the effect of PMNs on Tregs has not been investigated in the context of clinically
390 relevant vaccines, several studies have looked at the relationship between Tregs and PMNs in
391 models of inflammation and disease (Gao et al., 2015; Himmel et al., 2011; Lewkowicz et al.,
392 2013; Mishalian et al., 2014; Nadkarni et al., 2016; Perobelli et al., 2016; Richards et al., 2010).
393 Here we report that PMNs can inhibit Tregs, which is in contrast to prior work demonstrating that
394 PMNs promote Tregs in models where high level of inflammation is induced (Gao et al., 2015;
395 Mishalian et al., 2014; Perobelli et al., 2016). The exact way by which PMNs inhibit Tregs in
396 response to PCV remains to be elucidated, however multiple mechanisms could be involved.
397 Some possibilities could be via control of the transcription factor FOXP3, a master regulator of
398 Treg induction and function (Fontenot et al., 2003; Ono, 2020) or control of cytokines required for
399 Treg differentiation and viability. In traumatic brain injury patients, release of serine proteases
400 (neutrophil elastase and proteinase 3) by infiltrating PMNs cleaved cytokine receptors on the
401 surface of T cells including IL-2Rα, the IL-2 receptor subunit that is important for IL-2 signaling in
402 Tregs (Bank et al., 1999; Harris et al., 2023). In addition, those proteases can cleave cytokines
403 themselves including TGFβ and IL-2, leading to limited activation of T cell response (Ariel et al.,
404 1998; Fu et al., 2020). In response to PCV, PMNs may similarly inhibit Treg induction by release
405 of their proteases to deplete Treg-inducing cytokines and/or their respective receptors on the
406 surface of Tregs. Signaling of retinoic acid (RA) in naïve T cells enhances TGFβ-mediated
407 induction of Tregs (Ohkura et al., 2011) and RA boosts PMN anti-bacterial functions (Stream et
408 al., 2024). It is possible that RA sequestration by PMNs limits its availability for Treg induction.
409 PMNs could also be inhibiting Tregs through release of their granule component cathelicidin
410 antimicrobial peptide, the human form of which (LL-37) was shown to induce Treg apoptosis *in*
411 *vitro* (Mader et al., 2011). Alternatively, PMNs could be suppressing Tregs through the release
412 of miRNA containing extracellular vesicles (EVs). PMN-derived EVs containing miRNAs have

413 been shown to modulate responses in other cells including macrophages and endothelial cells
414 (Glemain et al., 2022; Gomez et al., 2020; Jiao et al., 2021). The absence of miRNA-146a has
415 been shown to promote Treg expansion, and other miRNAs are known to control Treg induction
416 (Kunze-Schumacher and Krueger, 2020; Lu et al., 2021a). PMNs, which express miRNA-146a
417 among others (Arroyo et al., 2021; Garley et al., 2024), could use such mechanism to limit Treg
418 expansion. All these potential mechanisms can be avenues of future research for this work.

419 The findings here suggest that the expanded Tregs in PMN-depleted mice are detrimental
420 and contribute to the defective antibody responses. In general, Tregs have been shown to
421 negatively affect immune responses to vaccines. Depletion of Tregs using αCD25 in vaccination
422 models against herpes simplex virus (HSV) and *Plasmodium berghei*, increased $CD8^+$ T cell
423 responses to their respective vaccine epitopes and led to increase protection against subsequent
424 challenge with the respective pathogens (Moore et al., 2005; Toka et al., 2004). In humans,
425 responses to an experimental vaccine of dendritic cells loaded with HIV peptides (Levy et al.,
426 2014) found that patients with lower levels of HIV-specific Tregs displayed better T-effector cell
427 responses following vaccination (Brezar et al., 2015). In the context of *S. pneumoniae*, blocking
428 of CTLA-4, an effector molecule on Tregs, enhanced levels of antibodies against pneumococcal
429 polysaccharides in immunized mice and higher Tregs in older adults were associated with
430 decreased proliferation of $CD4^+$ effector T cells in response to the pneumococcal protein AliB
431 (Boudewijns et al., 2005; He et al., 2021). Additionally, Tfrs, which we found are increased in
432 PCV-vaccinated PMN-depleted mice, have been shown to inhibit B cells responses and promote
433 the contraction of GC reactions (Jacobsen et al., 2021; Sage et al., 2016). The findings here,
434 showing an improvement of vaccine response upon depletion of the expanded Tregs in PMN-
435 depleted mice, are in line with the reported inhibitory role of Tregs in vaccine responses.

436 There have been several studies examining how Tregs and Tfrs inhibit B cell responses
437 (Wang and Zheng, 2013). They can affect B cell number, differentiation, and antibody responses
438 via release of soluble mediators such as the neuropeptide neuritin, IL-10 and TGFβ or through

439 contact dependent mechanisms involving CTLA4, PD1 and granzymes (Gonzalez-Figueroa et
440 al., 2021; Tan et al., 2022; Wang and Zheng, 2013). This suppression can lead to a decrease in
441 B cell expression of activation-induced deaminase (AID) (Lim et al., 2005). However, B cell
442 numbers and AID expression were not affected in this study. It is possible that the DNA binding
443 capacity or the enzymatic activity of AID are affected instead. AID activity is regulated by its
444 phosphorylation status which can either enhance or inhibit its enzymatic activity, depending on
445 the amino acid being phosphorylated (McBride et al., 2008; Park, 2012) by protein Kinase A (PKA)
446 (Basu et al., 2005; Chaudhuri et al., 2004; Demorest et al., 2011; Gazumyan et al., 2011). It is
447 therefore possible for Tregs to be regulating AID phosphorylation in response to PCV, rather than
448 overall expression through modulation of cAMP as they have been shown to do in DCs and
449 effector T cells (Klein and Bopp, 2016).

450 We found that the phenotypes observed in the preclinical model are also found in human
451 participants, highlighting the clinical relevance of this work. Upon vaccination of healthy human
452 donors, PMNs in the circulation changed phenotype suggesting they are responsive to
453 vaccination. Using peripheral blood collected from donors after PCV vaccination for *in vitro*
454 cocultures, addition of PMNs to PBMCs lead to a reduction in $FOXP3^{+}$ T cells and their
455 proliferation, recapitulating the Treg inhibiting property of PMNs seen in the mouse models.
456 However, further clinical studies are needed to assess the *in vivo* role of PMNs in protecting
457 human hosts against pneumococcal disease, including linking PMN phenotype to antibody
458 responses. Nevertheless, these findings can impact the design of improved pneumococcal
459 vaccine formulations that offer better efficacy, especially in the more vulnerable populations.
460 Despite their availability, pneumococcal vaccines do not mitigate the growing global burden of *S.*
461 *pneumonia* infections (CDC, 2022; Wiemken et al., 2014; Wiese et al., 2016). This is due in part
462 to the fact that the vaccines do not protect all populations equally, where male donors and aged
463 individuals mount lower responses compared to female counterparts. Interestingly, Tregs are
464 reported to be higher in males compared to sex-matched females and higher in older adults

465 compared to younger people (Afshan et al., 2012; Raynor et al., 2012; Robinson et al., 2022). In
466 this work, we identified the role of the PMN-Treg axis in controlling antibody responses in females
467 that can be targeted for improvement of current vaccine formulations moving forward. While
468 further studies are needed to tease apart the specific mechanisms behind this inhibition of Tregs
469 by PMNs, the findings have important implications for development of future vaccine strategies to
470 improve efficacy to infections. Indeed, this PMN-Treg axis can be further studied in the context of
471 sex and age-driven differences in vaccine responses (Flanagan et al., 2017; Pollard and Bijker,
472 2021) and can be targeted to increase vaccination efficacy in the vulnerable older adults and male
473 populations. The exact mechanisms of Treg inhibition by PMNs need to be elucidated to pinpoint
474 what pathways or molecules to target specifically in the future.
475
476 **Limitations of the Study**
477 One limitation of the study is the focus on young adult females, both in preclinical mouse
478 work and in human participants. Neutrophil responses are known to be affected by both host age
479 and biological sex (Klein and Flanagan, 2016; Lu et al., 2021b; Simmons et al., 2021; Spitzer,
480 1999). Therefore, their role in vaccine-mediated responses may be different in the more
481 vulnerable male and aged hosts. Indeed, our prior work in preclinical models (Tchalla et al., 2024)
482 as well as data from human studies (Soneji and Metlay, 2011; Wagenvoort et al., 2017; Wiese et
483 al., 2016) found that PCV efficacy is lower in males compared to females and declines with host
484 age. Therefore, we decided to first focus on the hosts that are the most protected following
485 vaccination (young adult females) and characterize PMN responses in them first and move to less
486 protected hosts as a next step. Currently ongoing studies in our lab are exploring the effect of
487 aging and biological sex on PMN responses to PCV. Another limitation is, for human participants,
488 we are limited by access to cells in the circulation. Therefore, and are unable to examine the effect
489 of PMNs on secondary lymphoid organs. We attempted to address that by performing

490 PMN/PBMC co-cultures and were able to recapitulate the inhibitory effect of PMNs on Tregs that
491 we observed *in vivo* in preclinical studies.
492 Further by being limited to responses in the circulation, we are unable to test if PMN phenotype
493 is altered upon tissue entry in people. However, unlike in mice, the phenotype of circulating PMNs
494 in human participants did change in response to PCV administration, emphasizing differences in
495 PMN behaviors across species. Finally, although we identified that control of Tregs by PMNs is
496 one of the mechanisms by which they affect antibody responses to PCV, how they do so remain
497 an open question. In summary, despite the discussed limitations, this study revealed new insights
498 into how innate immunity controls adaptive responses, which has implications for future vaccine
499 design, highlighting the importance of taking PMN responses into consideration.
500

501 **RESOURCE AVAILABILITY**

502 **Lead contact**

503 Requests for further information and resources should be directed to and will be fulfilled by the
504 lead contact, Elsa Bou Ghanem (elsaboug@buffalo.edu).

505 **Materials availability**

506 The study did not generate new unique reagents.

507 **Data and code availability**

508 All data reported in this paper will be shared by the lead contact upon request. This paper does
509 not report original code. Any additional information required to reanalyze the data reported in this
510 paper is available from the lead contact upon request.
511

512 **ACKNOWLEDGMENTS**

513 This work was supported by National Institute of Health grant R01 AG068568-01A1 to ENBG,
514 Mark Diamond Research Funds to EYIT, and an AHA predoctoral fellowship to AB. The content

is solely the responsibility of the authors and does not necessarily represent the official views of the National Institutes of Health.

AUTHOR CONTRIBUTIONS

EYIT conducted research, acquired data, analyzed data, and wrote the manuscript. AB conducted research, acquired data, and analyzed data. AYK, EL, MB, MC conducted research and acquired data. EAW provided materials. ENBG designed the research studies, wrote, and edited the manuscript, and had responsibility for final content. All authors read and approved the manuscript.

DECLARATION OF INTEREST

The authors have declared that no conflict of interest exists.

SUPPLEMENTAL INFORMATION

Document S1. Figures S1–S24.

MATERIALS AND METHODS

Experimental Model and Study Participant Detail

Mice

Adult (10-12 weeks old) female C57BL/6 mice were purchased from The Jackson Laboratory (Bar Harbor, Maine). Our study focused on female hosts, as there is a well-documented sex-based difference in responses to PCV where females elicit higher antibody responses and are better protected from subsequent infection compared to males (de St Maurice et al., 2016; Tchalla et al., 2024; Wagenvoort et al., 2017). Therefore, we examined the mechanisms behind vaccine efficacy in the better protected hosts. Ongoing work in our lab is focused on sex-based difference in PMN responses in vaccinated hosts (Tchalla et al., 2024) which is beyond the scope of this study. Adult (10-16 weeks old) C57BL/6-Tg(Foxp3-DTR/EGFP)23.2Spar/Mmjax DEREG mice

541 were a kind gift from Elizabeth Wohlfert and have been previously described in detail (Jin et al.,
542 2017; Lahl et al., 2007). All mice were housed in a specific-pathogen-free environment at the
543 University at Buffalo Jacobs School of Medicine and Biomedical Sciences animal facility.
544
545 **Human participants**
546 Healthy unvaccinated female participants (24-29 years old) were recruited. Individuals who were
547 pregnant, had acute infections within the last 2 weeks, took medication 48 hours prior, had history
548 of chronic infections, had conditions that altered immunity (autoimmunity, on immune modulating
549 drugs, history of cancer) were excluded from the study. At the first visit (week 0), donors had their
550 blood drawn then were administered the Polysaccharide Conjugate Vaccine Prevnar 20 (Pfizer,
551 Wyeth Pharmaceuticals) intramuscularly as per manufacturer's instructions. At week 1 and 4
552 following vaccination, donors had their blood drawn for subsequent PMN phenotyping. Blood from
553 week 1 was also used for coculture assays. All blood was collected into tubes containing sodium
554 citrate and visits occurred in the morning (8AM-10AM) to control for circadian variations in PMN
555 phenotype (Casanova-Acebes et al., 2013). All enrolled participants signed approved informed
556 consent forms.
557
558 **Study approvals**
559 All work with mice was performed in accordance with the recommendations in the Guide for the
560 Care and Use of Laboratory Animals published by the National Institutes of Health. All procedures
561 were reviewed and approved by the University at Buffalo Institutional Animal Care and Use
562 Committee (IACUC), approval number MIC33018Y. All work with human donors was approved
563 by the University at Buffalo Human investigation Review Board (IRB), approval number
564 STUDY00007111.
565
566 **Method Details**

567 **Murine immunization and sera collection**

568 Mice were vaccinated intramuscularly with 50ul of the Polysaccharide Conjugate Vaccine Prevnar
569 13 (Wyeth Pharmaceuticals) into the caudal thigh muscle. 10ul of blood from each mouse was
570 collected from the tail at weeks 0, 2 and 4 following vaccination and used for assessment of
571 antibody titers. Sera from each mouse group were collected via cardiac puncture 4 weeks
572 following vaccination, pooled and aliquoted to assess antibody quantity and functions in
573 subsequent assays.

574

575 **Bacteria**

576 *Streptococcus pneumoniae* TIGR4 strain (serotype 4) was a kind gift from Andrew Camilli.
577 Bacteria were grown to mid-exponential phase in Todd–Hewitt broth (BD Biosciences)
578 supplemented with Oxyrase at 37°C/5% carbon dioxide, aliquoted in growth media supplemented
579 with 20% glycerol and saved at -80°C as previously described (Tchalla et al., 2024; Tchalla et al.,
580 2020). Prior to use, bacteria were thawed on ice, washed, and enumerated by serial dilution in
581 PBS followed by dribbled plating on Tryptic Soy Agar (TSA) plates supplemented with 5% sheep
582 blood (Northeast Laboratory Services).

583

584 **Murine neutrophil depletion**

585 Mice were injected intraperitoneally with 50μg of the Ly6G-depleting antibody IA8 or isotype IgG
586 control following the same schedule as shown in Fig. S2A and previously described (Tchalla et
587 al., 2020). PMN depletion in the spleen was assessed by a myeloperoxidase ELISA (Invitrogen)
588 as per manufacture's instruction (Tchalla et al., 2020).

589

590 **Murine regulatory T cell depletion**

591 B6 mice were treated intraperitoneally with 300μg of the CD25-depleting antibody PC-61.5.3 or
592 isotype IgG1 control following the schedule shown in Fig. S19A. DEREG mice were treated
593 intraperitoneally with 1μg of diphtheria toxin (Millipore) or DMSO as vehicle control following the
594 schedule shown in Fig. S21A. Depletion efficiency was assessed by flow cytometry (Fig. S19 &
595 S21B).
596
597 **Murine organ/tissue processing and flow cytometry**
598 Blood, spleens and/or vaccine draining lymph nodes (vLNs- inguinal and popliteal) were
599 harvested from euthanized mice. Single cell suspensions from spleens and vLNs were prepared
600 in RPMI 1640 media supplemented with 10% Fetal Bovine Serum. Following red blood cells lysis
601 with an in-house hypotonic solution (8.29g ammonium chloride, 1g sodium bicarbonate, 0.038g
602 trypsin/ethylenediaminetetraacetic acid (EDTA) and 1L of water), the remaining cells were
603 enumerated, incubated with Fc block (2.4G2), Live/Dead dye (Invitrogen) and stained with
604 additional antibodies in separate panels.
605 For PMNs, cells were stained with Ly6G (1A8), CD11b (M1/70), CXCR4 (2B11), CCR7
606 (4B12), CD80 (16-10A1), CD86 (GL1), CD11c (N418), MHC-II (M5/114.15.2), PD-L1 (MIH5),
607 CD39 (24DMS1) and/or CD73 (TY/11.8) antibodies followed by permeabilization with
608 Cytofix/Cytoperm (BD) and intracellular staining with ARG1 (A1exF5).
609 For B cells, cells were stained with CD45R/B220 (RA3-6B2), CD138 (281-2), CD95
610 (SA367H8), and CD38 (90) antibodies followed by permeabilization with Fix/Perm buffer from the
611 FOXP3/Transcription factor staining buffer set (eBioscience) and intracellular staining with AID
612 (Polyclonal, Bioss).
613 For T cells, cells were stained with CD4 (RM4-5), TCRβ (H57-597), CD11a (M17/4),
614 CD49d (R1-2), PD1 (J43) and/or CXCR5 (SPRCL5) antibodies followed by permeabilization with
615 Fix/Perm buffer from the FOXP3/Transcription factor staining buffer set (eBioscience) and

616 intracellular staining with FOXP3 (FJK-16s), RORγT (Q31-378), Tbet (eBio4B10) and GATA3
617 (L580-823).
618 For intracellular cytokine staining in PMNs, cells were incubated in Brefeldin A in RPMI
619 1640 media supplemented with 10% Fetal Bovine Serum and 1% Pen/Strep and stimulated with
620 $9x10^6$ CFU/well of heat-killed *S. pneumoniae* TIGR4 strain, 10µl/well of PCV, 100nM of phorbol-
621 12-myristate 13-acetate (PMA) or media alone for 3 hours. Cells were then washed and stained
622 extracellularly with Fc block, Live/Dead dye, Ly6G, and CD11b antibodies followed by intracellular
623 staining with IFNγ (XMG1.2) after permeabilization with Cytofix/Cytoperm (BD). For intracellular
624 cytokine staining in T cells, cells were incubated in Brefeldin A (BD) in RPMI 1640 media
625 supplemented with 10% Fetal Bovine Serum and 1% Pen/Strep and stimulated with a mix of 81nM
626 of PMA and 1.34µM of Ionomycin (Cell activation cocktail, Biolegend) or media alone for 2 hours.
627 Cells were then washed and stained extracellularly with Fc block, Live/Dead dye, CD4, TCRβ,
628 CD44 (IM7) and LAP (TW7-16B4) antibodies followed by intracellular staining with IFNγ
629 (XMG1.2), IL-17A (TC11-18H10), IL-4 (11B11) and IL-10 (JES5-16E3) antibodies after
630 permeabilization with Fix/Perm buffer from the FOXP3/Transcription factor staining buffer set
631 (eBioscience). Following staining, cells were washed with FACS buffer (HBSS, 1% FBS and 0.1%
632 sodium azide) and fluorescence was assessed using a BD Fortessa. At least 20,000 cells in the
633 live, $CD4^+TCR\beta^+$ and $B220^+$ cells gates respectively were collected and analyzed using the
634 FlowJo software.
635
636 **Murine antibody enzyme-linked immunosorbent assay**
637 Antibodies in sera were assessed using an ELISA assay as previously described (Bhalla et al.,
638 2021; Tchalla et al., 2020). Briefly, Nunc-maxisorp plates (Thermo Scientific) were coated at 4°C
639 overnight with type 4 Pneumococcal Polysaccharide (ATCC®) at 2µg/well. The next day, plates
640 were washed in PBS supplemented with 0.25% Tween (PBS/T) and sera preabsorbed with a

641 pneumococcal cell wall polysaccharide mixture (CWP-multi, Cederlane) were added to the plates.
642 After a 2-hour incubation, plates were washed and incubated with diluted horseradish peroxidase
643 (HRP) conjugated anti-mouse IgM (Invitrogen), IgG (Millipore Sigma) or IgG1, IgG2b, IgG2c or
644 IgG3 (Southern Biotech). One hour later, plates were washed, TMB substrate (Thermo Scientific)
645 was added, and absorbance was read at 650nm using a Biotek microplate reader for 10 minutes
646 at 1-minute intervals. Antibody units were calculated as a percentage of standard sera included
647 in each assay. Standard sera were obtained from mice that were intranasally inoculated with *S.*
648 *pneumoniae* serotype 4 weekly for 3 weeks and immunized with PCV at week 4.
649
650 **Murine IFNγ enzyme-linked immunosorbent assay**
651 Single cell suspension of splenocytes were prepared in 2ml of RPMI 1640 media supplemented
652 with 10% Fetal Bovine Serum. IFNγ concentrations were quantified using the Mouse IFNγ ELISA
653 kit (Invitrogen, KMC4021) per manufacturer's instructions.
654
655 **Murine IFNγ blocking *in vivo***
656 Mice were treated intraperitoneally with 200μg of the IFNγ-blocking antibody XMG1.2 or isotype
657 control following same schedule as neutrophil depletion shown in Fig. S2A.
658
659 **Murine cytokine/chemokine array**
660 Pan cytokines were assessed using the Proteome Profiler Mouse XL Cytokine Array kit (R&D,
661 ARY028) following the manufacturer's instructions as previously described (Tchalla et al., 2024)
662 . Briefly, single cell suspension of splenocytes were prepared in 2ml of RPMI 1640 media
663 supplemented with 10% Fetal Bovine Serum. Cell suspensions were aliquoted and saved at -
664 80°C. Samples were thawed on ice prior to use, lysed with Triton-X (VWR, 0694) and quantified
665 for protein concentrations using the Pierce BCA protein assay kit (Thermofisher, A55864) per the

666 manufacturer's instructions. All samples were brought to the same protein concentrations and
667 used for pan-cytokine assessment. Protein membranes were read using the BioRad ChemiDoc
668 MP Imaging System and the intensity for each dot on the blots was quantified using the
669 QuickSpots Image Analysis Software. The intensity values of each blot were blanked using their
670 respective buffer only controls. Intensity values across multiple blots were normalized using the
671 blot with the highest standard. Fold change of the values from vaccinated PMN-depleted mice
672 over those of vaccinated PMN-sufficient mice were calculated and log transformed.
673
674 **Murine splenocyte culture assays**
675 For mice, single cell suspension of splenocytes were prepared in 2ml of RPMI 1640 media
676 supplemented with 10% Fetal Bovine Serum one day post vaccination. To remove PMNs from
677 the obtained suspensions, splenocytes were stained with a PE labeled anti-Ly6G antibody and
678 treated using the EasySep™ Release Mouse PE Positive Selection Kit (StemCell) following
679 manufacturer's instruction. One million cells per conditions were used and treated with $5x10^7$ CFU
680 heat-killed *S. pneumoniae* or 1µl/ml αCD3 (positive control). Cells were cocultured for two days
681 before assessing percentages of Tregs.
682
683 **Antibody binding to the surface of *S. pneumoniae***
684 Sera collected 4-weeks post vaccination were used to assess antibody binding to *S. pneumoniae*
685 (TIGR4) as previously described (Tchalla et al., 2024; Tchalla et al., 2020). After 30 minutes of
686 incubation at 37°C, cells were washed with FACS buffer and labeled with an APC-tagged anti-
687 mouse IgG (polyclonal) antibody for 30 minutes on ice in the dark. Cells were then washed,
688 resuspended in FACS buffer and fluorescence was assessed using a BD Fortessa. At least
689 10,000 cells were analyzed using the FlowJo software.
690
691 **Murine opsonophagocytic killing assay (OPH)**

692 Neutrophils were isolated from the bone marrow of mice using density centrifugation with
693 Histopaque 1119 and Histopaque 1077 (Sigma) as previously described (Bhalla et al., 2021; Bou
694 Ghanem et al., 2015; Tchalla et al., 2020). Briefly, Neutrophils were resuspended in HBSS
695 (without Ca^{2+} or Mg^{2+}) media supplemented with 0.1% gelatin and used in the assay. Sera
696 collected 4-weeks post vaccination were incubated with *S. pneumoniae* TIGR4 for 5 minutes and
697 added to neutrophils in HBSS (with Ca^{2+} and Mg^{2+}). Following a 40-minute incubation at 37°C,
698 reactions were plated on TSA plates with 5% sheep blood. Percent killing was calculated relative
699 to a no neutrophils control for each sera condition.
700
701 **Murine adoptive transfer of sera**
702 Four weeks following immunization, naïve, vaccinated neutrophil- and Treg-sufficient, neutrophil-
703 depleted, neutrophils- and Treg-depleted and Treg-depleted were euthanized. Blood was
704 harvested via cardiac puncture; sera were obtained from the blood and pooled for each mouse
705 group. A volume of 250µL of sera was transferred intraperitoneally into naive recipients which
706 were infected 1hour later.
707
708 **Animal infections**
709 Mice were infected intratracheally with $3x10^5$ CFU of *S. pneumoniae* serotype 4 (TIGR4) using
710 the tongue pull method as previously described (Lenhard et al., 2022; Tchalla et al., 2020). Mice
711 were monitored for survival for a total of 7 days post infection and assessed daily for bacteremia
712 by plating blood collected in 50mM EDTA on blood agar plates for enumeration of bacterial CFU.
713
714 **Human PMN isolation and flow cytometry**
715 For participants, PMNs were isolated from peripheral blood of week 0, 1, 4 post vaccinated
716 donors using EasySep™ Direct Human Neutrophil Isolation Kit (StemCell) respectively following
717 manufacturers' instructions. For each donor and visit $1x10^5$ PMNs were added to each well and

718 then stained with CD16 (eBioCB16), CD14 (61D3), CD10 (MEM-78), HLA-DR (L243), CD86
719 (BU63), PD-L1 (MIH1), CD73 (AD2), and/or CD39 (eBioA1) antibodies followed by
720 permeabilization with Cytofix/Cytoperm (BD) and intracellular staining with ARG1 (A1exF5).
721 Following staining, cells were washed with FACS buffer and fluorescence was assessed using a
722 BD Fortessa. At least 5000 cells in the $CD16^+$ gate were collected and analyzed using the FlowJo
723 software.
724
725 **Human PMN FLOWSOM analysis**
726 Analysis and data visualization of the PMN phenotype with and without vaccination over time was
727 completed using a software OMIQ (Dotmatics). Traditional gating was done to differentiate the
728 neutrophil population and all the markers. Dimensional reduction was next performed with
729 optimized parameters for T-distributed stochastic neighbor embedding which improves
730 visualization of large datasets by reducing it to 2D/3D map while preserving local structure.
731 Clustering into neutrophil subsets was done using Flow-cytometry specific self-organizing map
732 (FLOWSOM)(Van Gassen et al., 2015) algorithm. Clustered heat maps were made based on
733 meta-cluster gating to characterize the different PMN subsets based on the expression of different
734 markers.
735
736 **Human PMN/PBMC coculture assays**
737 For participants, PBMCs and PMNs were isolated from peripheral blood of 1-week
738 vaccinated donors using the One-Step Polymorph (Accurate Chemical) and EasySep™ Direct
739 Human Neutrophil Isolation Kit (StemCell) respectively following manufacturers' instructions. For
740 each donor, $2x10^5$ PBMCs were incubated in (RPMI with 10% FBS) with or without addition of
741 $5x10^4$ PMNs and stimulated with 10µl of PCV. Cells were cocultured for two days before
742 assessing percentages and proliferation of T cells**.** At 48 hours post incubation, T cells were
743 stained with CD11a (HI111), PD1(EH12.1), CD4(S3.5), CD49d (9F10) and CXCR5 (MU5UBEE)

744 followed by permeabilization with Fix/Perm buffer from the FOXP3/Transcription factor staining
745 buffer set (eBioscience) and intracellular staining with FOXP3 (PCH101), RORγT (AFJKS-9), Tbet
746 (eB4B10), GATA3 (L580-823) and Ki67 (B56). Following staining, cells were washed with FACS
747 buffer and data collected using a BD Fortessa. At least 10,000 cells in the live $CD4^+$ gate were
748 collected and analyzed using the FlowJo software.
749
750 **Quantification and statistical analysis**
751 All statistical analysis was done using GraphPad Prism version 11 software. Data were checked
752 for normality distribution using the Shapiro-Wilk test. Significant differences were determined by
753 One-way analysis of variance followed Šídák's, Holm-Šídák's, Tukey's or Dunnett's multiple
754 comparisons test; Kruskal-Wallis One-way analysis of variance followed Dunn's multiple
755 comparisons; Student's t test; or one sample t-test as appropriate. Survival was analyzed using
756 the log-rank (Mantel-Cox) test. All p values <0.05 were considered significant.
757
758
759
760
761
762
763
764
765
766
767
768
769

770 **FIGURE TITLES AND LEGENDS**

A. Migration markers expression on circulating PMNs

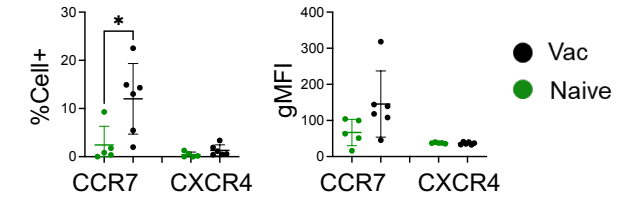

B. PMN influx

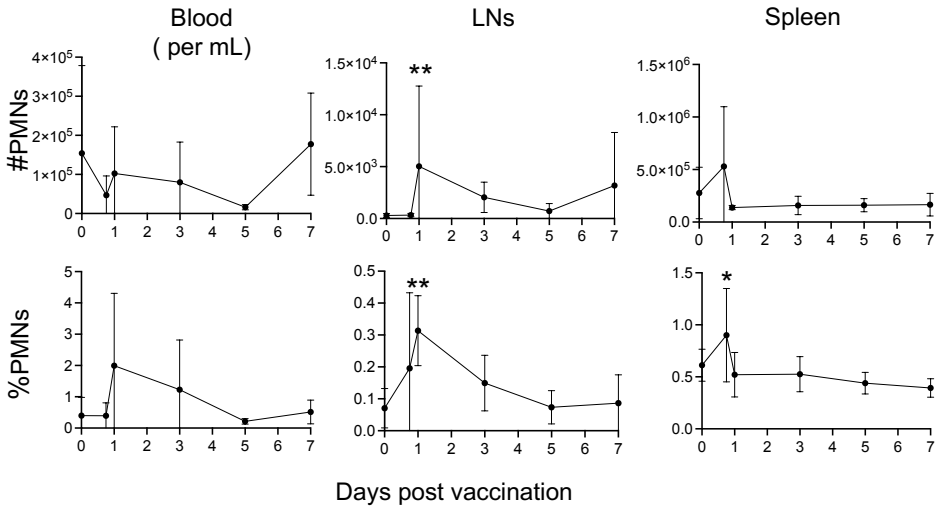

C. PMN phenotype

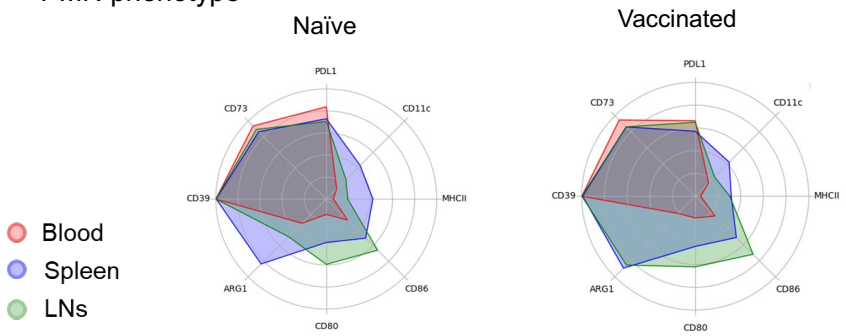

771

772 **Figure 1: PMN migration to secondary lymphoid organs following vaccination.** Adult
773 C57BL/6 female mice were injected with PCV or PBS. (A) Blood was collected from the mice 24
774 hours following vaccination and assessed using flow cytometry. Percentages (left) and gMFI
775 (right) of CCR7 and CXCR4 on live PMNs ($Ly6G^{+}CD11b^{+}$) were determined. (B) At different
776 timepoints post vaccination, blood, spleen and vLNs were collected from all mice and live PMN

777 (Ly6G^{+}CD11b^{+}) numbers (top) and percentages (bottom) was assessed using flow cytometry. (C)
778 Post vaccination, blood, spleen and vLNs were collected and percent expression of various
779 markers on PMNs were assessed by flow cytometry. Expression of MHC-II PD-L1, ARG1, CD73
780 and CD39, CD80, CD86 and CD11c were assessed 18-24 hours post vaccination. Data show
781 percent expression of markers on PMNs in all organs/tissue overlayed for naïve and vaccinated
782 mice. (A) Data are pooled from 3 separate experiments and each dot represents an individual
783 mouse with a total of n=5 naïve and n=6 vaccinated mice. Graphs represent the mean +/- SD. *
784 denotes significant differences between the indicated groups as determined by One-way ANOVA
785 followed by Sidak's multiple comparisons test. * is $p \leq 0.05$. (B) Data are pooled from 3 separate
786 experiments with a total of 6 mice per timepoint. Line graphs represent the mean +/- 95%
787 confidence interval. * denotes significant differences between the indicated groups as determined
788 by Kruskal-Wallis test followed by Dunn's multiple comparisons test. * is $p \leq 0.05$ and ** is $p \leq 0.01$.
789 (C) Data are pooled from 3 separate experiments with a total of n=5 naïve and n=6 vaccinated
790 mice and are presented as radar plots generated using R studio. Abbreviations: gMFI = geometric
791 Mean Fluorescence Intensity, MHC = Major Histocompatibility Complex.
792

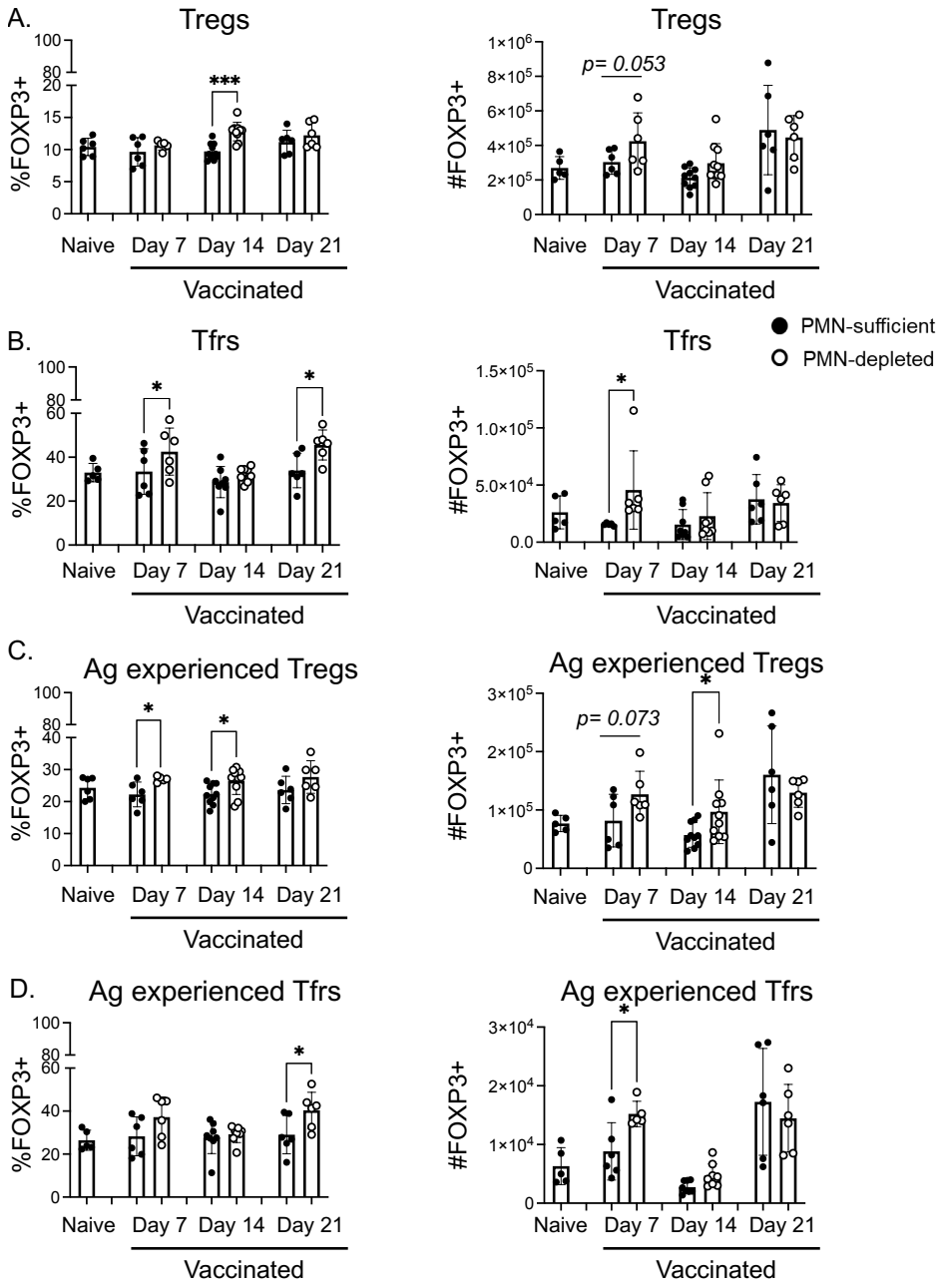

Figure 2: Effect of PMN depletion on regulatory T cells. Adult C57BL/6 female mice were injected with PCV or PBS and depleted of their PMNs or treated with an isotype control. Spleens were collected from all mice and assessed using flow cytometry on days 7, 14 and 21 post vaccination. (A-B) Live total ($CD4^+TCR\beta^+$) and (C-D) antigen experienced ($CD11a^+CD49d^+$) T cells were gated on. Percentages (left) and numbers (right) of (A&C) regulatory T cells ($FOXP3^+$)

800 and (B&D) T follicular regulatory T cells ($CXCR5^{+}PD1^{+}$ $FOXP3^{+}$) were determined from the total
801 and antigen experienced T cell gates. Data are pooled from 4 separate experiments and each dot
802 represents an individual mouse with a total of n=6 naïve, n=6 vaccinated day 7, n=8-10 vaccinated
803 day 14, and n=6 vaccinated day 21 mice per group. * denotes significant differences between the
804 indicated groups as determined by One-way ANOVA followed by Sidak's multiple comparisons
805 test. * is $p \leq 0.05$ and *** is $p \leq 0.001$. Bar graphs represent the mean +/- SD.
806
807
808
809
810
811
812
813
814
815
816
817

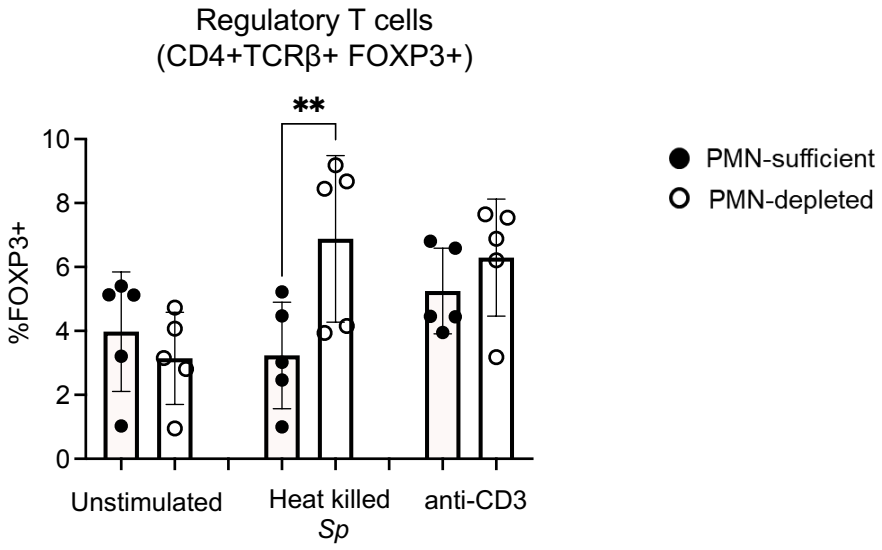

818

819

820 **Figure 3: Effect of PMN depletion on Tregs in mice *in vitro.*** Adult C57BL/6 female mice were
821 injected with PCV or PBS and depleted of their PMNs or treated with an isotype control. On day
822 1 post vaccination, splenocytes were isolated and cultured in the presence or absence of PMNs
823 for 2 days with heat-killed *S. pneumoniae* or αCD3 as stimulants. Percentage of $FOXP3^+$ cells
824 were determined in the live $CD4^+$ cells gate is shown. Data are pooled from separate experiments.
825 * denotes significant differences between the indicated groups as determined by One-Way
826 ANOVA followed by Šídák's multiple comparisons test. ** is $p \leq 0.01$. Graphs represent the mean
827 +/- SD.

828

829

830

831

832

833

834

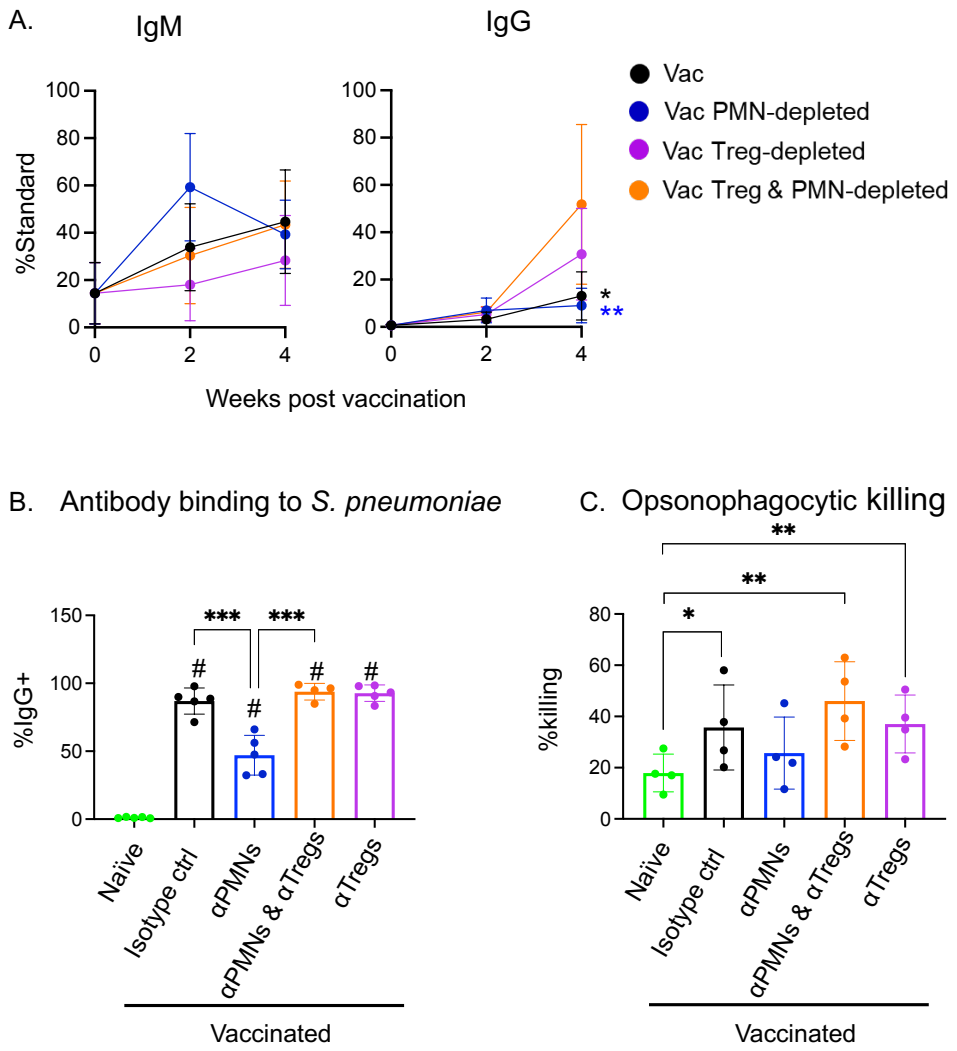

Figure 4: Effect of Treg depletion on antibody responses. Adult C57BL/6 female mice were injected with PCV or PBS and depleted of their PMNs and/or Tregs (αCD25) or treated with an isotype control. (A) Production of IgM and total IgG against type 4 pneumococcal polysaccharides were assessed on weeks 0, 2 and 4 post vaccination. Sera collected 4-weeks post vaccination were used to assess (B) the binding efficacy of antibodies to *S. pneumoniae* using flow cytometry and (C) the ability of antibodies to induce opsonophagocytic killing by PMNs. (A) Data are presented as percentage of standard sera and are pooled from a total of 3 experiments with a total of n=9 mice per group per timepoint. * denotes significant differences between PMNs- & Tregs-depleted mice and group matching the symbol color as determined by Kruskal-Wallis test

845 followed by Dunn's multiple comparisons test. (B) Data are from 5 separate experiments with
846 each dot representing the average of technical replicates. * denotes significant differences
847 between the indicated groups as determined by One-way ANOVA followed by Šídák's multiple
848 comparisons test and # denotes significant differences from naïve as determined by One-way
849 ANOVA followed by Holm-Šídák's multiple comparisons test. *** is $p \leq 0.001$, and # is $p \leq 0.001$.
850 Bar graphs represent the mean +/- SD. (C) Data are pooled from 3 separate experiments with
851 each dot representing the average of technical replicates from an individual mouse. * denotes
852 significant differences between the indicated groups as determined by One-way ANOVA followed
853 by Šídák's multiple comparisons test. * is $p \leq 0.05$ and ** is $p \leq 0.01$. All line graphs represent the
854 mean +/- 95% confidence interval and all bar graphs represent the mean +/- SD.
855
856
857
858
859
860
861
862
863
864
865
866
867
868
869
870

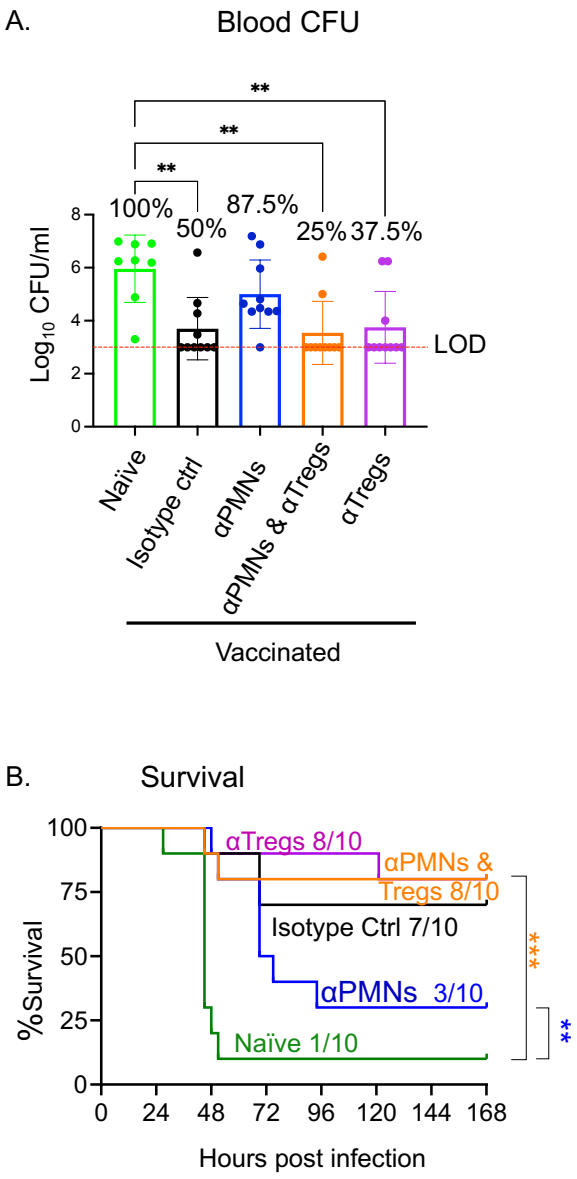

871

872 **Figure 5: Effect of Treg depletion on the protective efficacy of sera against pneumococcal**
873 **infection.** Adult C57BL/6 female mice were injected with PCV or PBS and depleted of their PMNs
874 and/or Tregs (αCD25) or treated with an isotype control. Sera were collected from all mice 4
875 weeks post vaccination. Sera from each mouse group was adoptively transferred into a new set
876 of naïve mice which were subsequently infected with $3x10^5$ CFU of *S. pneumoniae*. (A) Bacterial
877 burden in the blood was assessed 45 hours post infection. (B) All mice were monitored for survival
878 for 7 days following infection. (A) Data are pooled from 2 separate experiments and each dot
879 represents an individual mouse with a total of n=10 mice per group. * denotes significant

880 differences between the indicated groups as determined by Kruskal-Wallis test followed by Dunn's
881 multiple comparisons test. Bar graphs represent the mean +/- SD. (B) Data are pooled from 2
882 separate experiments with a total of n=10 mice per group. * denotes significant differences
883 between the indicated groups as determined by Mantel-Cox test. ** is $p \leq 0.01$, and ** is $p \leq 0.01$.
884
885
886
887
888
889
890
891
892
893
894
895
896
897
898
899
900
901
902
903
904
905

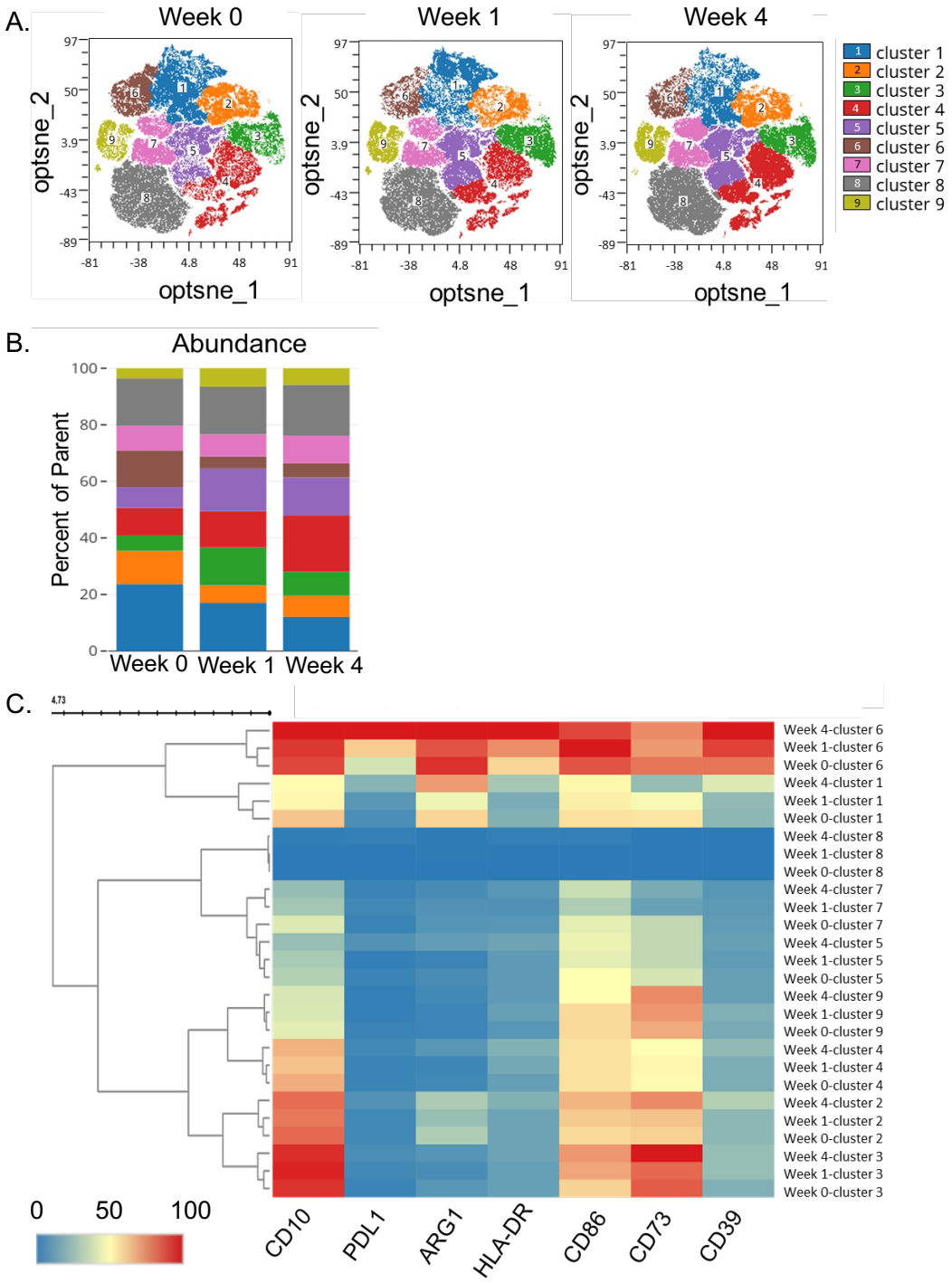

Figure 6: PMN phenotype following PCV vaccination in humans. Young (24-29 years old) female donors were vaccinated with PCV. Blood was collected prior (week 0) to and on weeks 1 & 4 post vaccination. PMNs were isolated from peripheral blood and assessed using flow

911 cytometry. Expressions of HLA-DR, CD10, CD86, PD-L1, ARG1, CD73 and CD39 on PMNs were
912 determined. (A) Clustering of investigated markers throughout the weeks, (B) cluster abundance
913 throughout the weeks, and (C) heat map of markers throughout the different weeks and clusters
914 were analyzed using FLOSOM via OMIQ. Data are pooled from six donors.
915
916
917
918
919
920
921
922
923
924
925
926
927
928
929
930
931
932
933
934
935
936

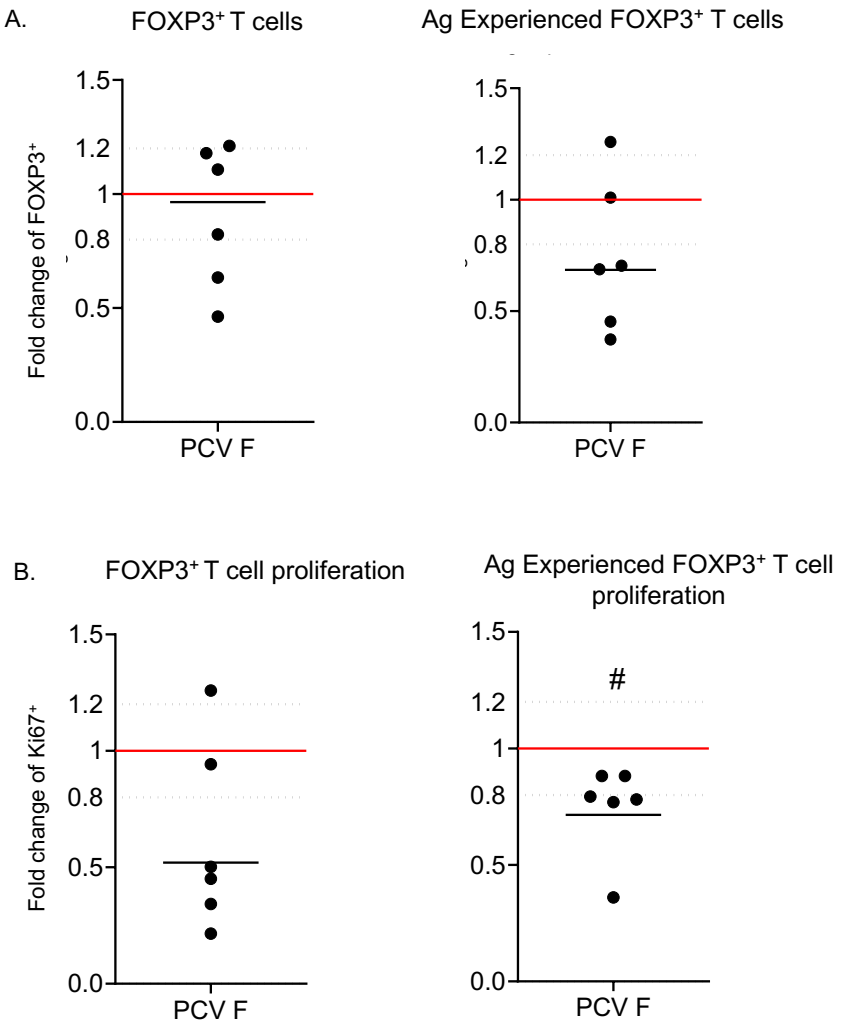

Figure 7: Human PMN and PBMC co-cultures following PCV vaccination. Young (24-29 years old) female donors were vaccinated with PCV. One week post vaccination, PBMCs and PMNs were isolated from peripheral blood. PBMCs were cultured in the presence or absence of matched donor PMNs for 2 days with PCV as a stimulant. Fold change of the percentages of (A) $FOXP3^+$ and (B) $Ki67^+$ $FOXP3^+$ cells gated from total (left) and antigen experienced (right) $CD4^+$ T cells are shown. Data are pooled from six donors and each dot represents a donor. Data are presented as fold change of PBMC divided by PBMC +PMNs conditions. The dashed lines represent a 20% difference in responses between the conditions. Graphs represent the mean, and # indicate significant differences from 1 as measured by a one-sample t-test.

REFERENCES

Abbas, A.K., Burstein, H.J., and Bogen, S.A. (1993). Determinants of helper T cell-dependent antibody production. Semin Immunol *5*, 441-447.

Abi Abdallah, D.S., Egan, C.E., Butcher, B.A., and Denkers, E.Y. (2011). Mouse neutrophils are professional antigen-presenting cells programmed to instruct Th1 and Th17 T-cell differentiation. International immunology *23*, 317-326.

Afshan, G., Afzal, N., and Qureshi, S. (2012). CD4+CD25(hi) regulatory T cells in healthy males and females mediate gender difference in the prevalence of autoimmune diseases. Clin Lab *58*, 567-571.

Allard, B., Longhi, M.S., Robson, S.C., and Stagg, J. (2017). The ectonucleotidases CD39 and CD73: Novel checkpoint inhibitor targets. Immunol Rev *276*, 121-144.

Areström, I., Zuber, B., Bengtsson, T., and Ahlborg, N. (2012). Measurement of human latent Transforming Growth Factor-β1 using a latency associated protein-reactive ELISA. J Immunol Methods *379*, 23-29.

Ariel, A., Yavin, E.J., Hershkoviz, R., Avron, A., Franitza, S., Hardan, I., Cahalon, L., Fridkin, M., and Lider, O. (1998). IL-2 induces T cell adherence to extracellular matrix: inhibition of adherence and migration by IL-2 peptides generated by leukocyte elastase. Journal of immunology *161*, 2465-2472.

Arroyo, A.B., Fernandez-Perez, M.P., Del Monte, A., Aguila, S., Mendez, R., Hernandez-Antolin, R., Garcia-Barber, N., de Los Reyes-Garcia, A.M., Gonzalez-Jimenez, P., Arcas, M.I.*, et al.* (2021). miR-146a is a pivotal regulator of neutrophil extracellular trap formation promoting thrombosis. Haematologica *106*, 1636-1646.

Ballesteros, I., Rubio-Ponce, A., Genua, M., Lusito, E., Kwok, I., Fernandez-Calvo, G., Khoyratty, T.E., van Grinsven, E., Gonzalez-Hernandez, S., Nicolas-Avila, J.A.*, et al.* (2020). Co-option of Neutrophil Fates by Tissue Environments. Cell *183*, 1282-1297 e1218.

Bank, U., Reinhold, D., Schneemilch, C., Kunz, D., Synowitz, H.J., and Ansorge, S. (1999). Selective proteolytic cleavage of IL-2 receptor and IL-6 receptor ligand binding chains by neutrophil-derived serine proteases at foci of inflammation. Journal of interferon & cytokine research : the official journal of the International Society for Interferon and Cytokine Research *19*, 1277-1287.

Basu, U., Chaudhuri, J., Alpert, C., Dutt, S., Ranganath, S., Li, G., Schrum, J.P., Manis, J.P., and Alt, F.W. (2005). The AID antibody diversification enzyme is regulated by protein kinase A phosphorylation. Nature *438*, 508-511.

Bayry, J. (2014). Regulatory T cells as adjuvant target for enhancing the viral disease vaccine efficacy. Virusdisease *25*, 18-25.

Beauvillain, C., Cunin, P., Doni, A., Scotet, M., Jaillon, S., Loiry, M.L., Magistrelli, G., Masternak, K., Chevailler, A., Delneste, Y.*, et al.* (2011). CCR7 is involved in the migration of neutrophils to lymph nodes. Blood *117*, 1196-1204.

Bert, S., Nadkarni, S., and Perretti, M. (2023). Neutrophil-T cell crosstalk and the control of the host inflammatory response. Immunol Rev *314*, 36-49.

Bhalla, M., Nayerhoda, R., Tchalla, E.Y.I., Abamonte, A., Park, D., Simmons, S.R., Pfeifer, B.A., and Bou Ghanem, E.N. (2021). Liposomal Encapsulation of Polysaccharides (LEPS) as an Effective Vaccine Strategy to Protect Aged Hosts Against S. pneumoniae Infection. Frontiers in Aging *2*.

Bhattacharya, P., Dey, R., Saxena, A., Karmakar, S., Ismail, N., Gannavaram, S., Dagur, P.K., Satoskar, M., Satoskar, S., De Paoli, S.*, et al.* (2020). Essential Role of Neutrophils in the Protective Immune Response Induced by a Live Attenuated Leishmania Vaccine. Journal of immunology *205*, 3333-3347.

996 Bird, A.K., Chang, M., Barnard, J., Goldman, B.I., Meednu, N., Rangel-Moreno, J., and Anolik,
997 J.H. (2017). Neutrophils Slow Disease Progression in Murine Lupus via Modulation of
998 Autoreactive Germinal Centers. The Journal of Immunology *199*, 458-466.
999 Bou Ghanem, E.N., Clark, S., Roggensack, S.E., McIver, S.R., Alcaide, P., Haydon, P.G., and
1000 Leong, J.M. (2015). Extracellular Adenosine Protects against Streptococcus pneumoniae Lung
1001 Infection by Regulating Pulmonary Neutrophil Recruitment. PLoS Pathog *11*, e1005126.
1002 Boudewijns, M., Jeurissen, A., Wuyts, M., Moens, L., Boon, L., Van Neerven, J.J., Kasran, A.,
1003 Overbergh, L., Lenaerts, C., Waer, M.*, et al.* (2005). Blockade of CTLA-4 (CD152) enhances the
1004 murine antibody response to pneumococcal capsular polysaccharides. J Leukoc Biol *78*, 1060-
1005 1069.
1006 Brezar, V., Ruffin, N., Richert, L., Surenaud, M., Lacabaratz, C., Palucka, K., Thiebaut, R.,
1007 Banchereau, J., Levy, Y., and Seddiki, N. (2015). Decreased HIV-specific T-regulatory responses
1008 are associated with effective DC-vaccine induced immunity. PLoS Pathog *11*, e1004752.
1009 Casanova-Acebes, M., Pitaval, C., Weiss, L.A., Nombela-Arrieta, C., Chèvre, R., N, A.G.,
1010 Kunisaki, Y., Zhang, D., van Rooijen, N., Silberstein, L.E.*, et al.* (2013). Rhythmic modulation of
1011 the hematopoietic niche through neutrophil clearance. Cell *153*, 1025-1035.
1012 CDC (2022). Center for Disease Control and Prevention. Active Bacterial Core Surveillance
1013 Report, Emerging Infections Program Network, Streptococcus pneumoniae.
1014 Chaudhuri, J., Khuong, C., and Alt, F.W. (2004). Replication protein A interacts with AID to
1015 promote deamination of somatic hypermutation targets. Nature *430*, 992-998.
1016 Chorny, A., Casas-Recasens, S., Sintes, J., Shan, M., Polentarutti, N., Garcia-Escudero, R.,
1017 Walland, A.C., Yeiser, J.R., Cassis, L., Carrillo, J.*, et al.* (2016). The soluble pattern recognition
1018 receptor PTX3 links humoral innate and adaptive immune responses by helping marginal zone B
1019 cells. The Journal of experimental medicine *213*, 2167-2185.
1020 Christiaansen, A.F., Dixit, U.G., Coler, R.N., Marie Beckmann, A., Reed, S.G., Winokur, P.L.,
1021 Zimmerman, M.B., Varga, S.M., and Wilson, M.E. (2017). CD11a and CD49d enhance the
1022 detection of antigen-specific T cells following human vaccination. Vaccine *35*, 4255-4261.
1023 Culshaw, S., Millington, O.R., Brewer, J.M., and McInnes, I.B. (2008). Murine neutrophils present
1024 Class II restricted antigen. Immunology letters *118*, 49-54.
1025 de Kleijn, S., Langereis, J.D., Leentjens, J., Kox, M., Netea, M.G., Koenderman, L., Ferwerda, G.,
1026 Pickkers, P., and Hermans, P.W. (2013). IFN-γ-stimulated neutrophils suppress lymphocyte
1027 proliferation through expression of PD-L1. PLoS One *8*, e72249.
1028 De Silva, N.S., and Klein, U. (2015). Dynamics of B cells in germinal centres. Nature reviews
1029 Immunology *15*, 137-148.
1030 de St Maurice, A., Schaffner, W., Griffin, M.R., Halasa, N., and Grijalva, C.G. (2016). Persistent
1031 Sex Disparities in Invasive Pneumococcal Diseases in the Conjugate Vaccine Era. J Infect Dis
1032 *214*, 792-797.
1033 Demorest, Z.L., Li, M., and Harris, R.S. (2011). Phosphorylation directly regulates the intrinsic
1034 DNA cytidine deaminase activity of activation-induced deaminase and APOBEC3G protein. J Biol
1035 Chem *286*, 26568-26575.
1036 Di Noia, J.M., and Neuberger, M.S. (2007). Molecular mechanisms of antibody somatic
1037 hypermutation. Annu Rev Biochem *76*, 1-22.
1038 Dong, C. (2021). Cytokine Regulation and Function in T Cells. Annual review of immunology *39*,
1039 51-76.
1040 Farkas, A.M., Marvel, D.M., and Finn, O.J. (2013). Antigen choice determines vaccine-induced
1041 generation of immunogenic versus tolerogenic dendritic cells that are marked by differential
1042 expression of pancreatic enzymes. Journal of immunology *190*, 3319-3327.
1043 Flanagan, K.L., Fink, A.L., Plebanski, M., and Klein, S.L. (2017). Sex and Gender Differences in
1044 the Outcomes of Vaccination over the Life Course. Annu Rev Cell Dev Biol *33*, 577-599.
1045 Fontenot, J.D., Gavin, M.A., and Rudensky, A.Y. (2003). Foxp3 programs the development and
1046 function of CD4+CD25+ regulatory T cells. Nature immunology *4*, 330-336.

1047 Forthal, D.N. (2014). Functions of Antibodies. Microbiol Spectr *2*, 1-17.
1048 Fu, Z., Akula, S., Thorpe, M., and Hellman, L. (2020). Potent and Broad but not Unselective
1049 Cleavage of Cytokines and Chemokines by Human Neutrophil Elastase and Proteinase 3. Int J
1050 Mol Sci *21*.
1051 Gao, Y., Min, K., Zhang, Y., Su, J., Greenwood, M., and Gronert, K. (2015). Female-Specific
1052 Downregulation of Tissue Polymorphonuclear Neutrophils Drives Impaired Regulatory T Cell and
1053 Amplified Effector T Cell Responses in Autoimmune Dry Eye Disease. Journal of immunology
1054 *195*, 3086-3099.
1055 Garley, M., Nowak, K., and Jablonska, E. (2024). Neutrophil microRNAs. Biol Rev Camb Philos
1056 Soc *99*, 864-877.
1057 Gazumyan, A., Timachova, K., Yuen, G., Siden, E., Di Virgilio, M., Woo, E.M., Chait, B.T., Reina
1058 San-Martin, B., Nussenzweig, M.C., and McBride, K.M. (2011). Amino-terminal phosphorylation
1059 of activation-induced cytidine deaminase suppresses c-myc/IgH translocation. Mol Cell Biol *31*,
1060 442-449.
1061 Glemain, A., Neel, M., Neel, A., Andre-Gregoire, G., Gavard, J., Martinet, B., Le Bloas, R., Riquin,
1062 K., Hamidou, M., Fakhouri, F.*, et al.* (2022). Neutrophil-derived extracellular vesicles induce
1063 endothelial inflammation and damage through the transfer of miRNAs. J Autoimmun *129*, 102826.
1064 Gomez, I., Ward, B., Souilhol, C., Recarti, C., Ariaans, M., Johnston, J., Burnett, A., Mahmoud,
1065 M., Luong, L.A., West, L.*, et al.* (2020). Neutrophil microvesicles drive atherosclerosis by
1066 delivering miR-155 to atheroprone endothelium. Nat Commun *11*, 214.
1067 Gonzalez-Figueroa, P., Roco, J.A., Papa, I., Nunez Villacis, L., Stanley, M., Linterman, M.A.,
1068 Dent, A., Canete, P.F., and Vinuesa, C.G. (2021). Follicular regulatory T cells produce neuritin to
1069 regulate B cells. Cell *184*, 1775-1789 e1719.
1070 Hampton, H.R., Bailey, J., Tomura, M., Brink, R., and Chtanova, T. (2015). Microbe-dependent
1071 lymphatic migration of neutrophils modulates lymphocyte proliferation in lymph nodes. Nat
1072 Commun *6*, 7139.
1073 Harris, F., Berdugo, Y.A., and Tree, T. (2023). IL-2-based approaches to Treg enhancement. Clin
1074 Exp Immunol *211*, 149-163.
1075 He, S.W.J., van de Garde, M.D.B., Pieren, D.K.J., Poelen, M.C.M., Voss, F., Abdullah, M.R.,
1076 Hammerschmidt, S., and van Els, C. (2021). Diminished Pneumococcal-Specific CD4(+) T-Cell
1077 Response is Associated With Increased Regulatory T Cells at Older Age. Front Aging *2*, 746295.
1078 Himmel, M.E., Crome, S.Q., Ivison, S., Piccirillo, C., Steiner, T.S., and Levings, M.K. (2011).
1079 Human CD4+ FOXP3+ regulatory T cells produce CXCL8 and recruit neutrophils. Eur J Immunol
1080 *41*, 306-312.
1081 Jacobsen, J.T., Hu, W., TB, R.C., Solem, S., Galante, A., Lin, Z., Allon, S.J., Mesin, L., Bilate,
1082 A.M., Schiepers, A.*, et al.* (2021). Expression of Foxp3 by T follicular helper cells in end-stage
1083 germinal centers. Science *373*.
1084 Jee, J., Bonnegarde-Bernard, A., Duverger, A., Iwakura, Y., Cormet-Boyaka, E., Martin, T.L.,
1085 Steiner, H.E., Bachman, R.C., and Boyaka, P.N. (2015). Neutrophils negatively regulate induction
1086 of mucosal IgA responses after sublingual immunization. Mucosal Immunol *8*, 735-745.
1087 Jiang, X., Wu, X., Xiao, Y., Wang, P., Zheng, J., Wu, X., and Jin, Z. (2023). The ectonucleotidases
1088 CD39 and CD73 on T cells: The new pillar of hematological malignancy. Front Immunol *14*,
1089 1110325.
1090 Jiao, Y., Zhang, T., Zhang, C., Ji, H., Tong, X., Xia, R., Wang, W., Ma, Z., and Shi, X. (2021).
1091 Exosomal miR-30d-5p of neutrophils induces M1 macrophage polarization and primes
1092 macrophage pyroptosis in sepsis-related acute lung injury. Crit Care *25*, 356.
1093 Jin, R.M., Blair, S.J., Warunek, J., Heffner, R.R., Blader, I.J., and Wohlfert, E.A. (2017).
1094 Regulatory T Cells Promote Myositis and Muscle Damage in Toxoplasma gondii Infection. Journal
1095 of immunology *198*, 352-362.

1096 Kamenyeva, O., Boularan, C., Kabat, J., Cheung, G.Y.C., Cicala, C., Yeh, A.J., Chan, J.L.,
1097 Periasamy, S., Otto, M., and Kehrl, J.H. (2015). Neutrophil Recruitment to Lymph Nodes Limits
1098 Local Humoral Response to Staphylococcus aureus. PLOS Pathogens *11*, e1004827.
1099 Karachunski, P.I., Ostlie, N.S., Monfardini, C., and Conti-Fine, B.M. (2000). Absence of IFN-γ or
1100 IL-12 Has Different Effects on Experimental Myasthenia Gravis in C57BL/6 Mice. The Journal of
1101 Immunology *164*, 5236-5244.
1102 Kasten, K.R., Muenzer, J.T., and Caldwell, C.C. (2010). Neutrophils are significant producers of
1103 IL-10 during sepsis. Biochemical and Biophysical Research Communications *393*, 28-31.
1104 Klein, M., and Bopp, T. (2016). Cyclic AMP Represents a Crucial Component of Treg Cell-
1105 Mediated Immune Regulation. Front Immunol *7*, 315.
1106 Klein, S.L., and Flanagan, K.L. (2016). Sex differences in immune responses. Nature reviews
1107 Immunology *16*, 626-638.
1108 Kunze-Schumacher, H., and Krueger, A. (2020). The Role of MicroRNAs in Development and
1109 Function of Regulatory T Cells - Lessons for a Better Understanding of MicroRNA Biology. Front
1110 Immunol *11*, 2185.
1111 Lahl, K., Loddenkemper, C., Drouin, C., Freyer, J., Arnason, J., Eberl, G., Hamann, A., Wagner,
1112 H., Huehn, J., and Sparwasser, T. (2007). Selective depletion of Foxp3+ regulatory T cells
1113 induces a scurfy-like disease. The Journal of experimental medicine *204*, 57-63.
1114 Leliefeld, P.H.C., Koenderman, L., and Pillay, J. (2015). How Neutrophils Shape Adaptive
1115 Immune Responses. Frontiers in Immunology *6*.
1116 Lenhard, A., Joma, B.H., Siwapornchai, N., Hakansson, A.P., Leong, J.M., and Bou Ghanem,
1117 E.N. (2022). A Mouse Model for the Transition of Streptococcus pneumoniae from Colonizer to
1118 Pathogen upon Viral Co-Infection Recapitulates Age-Exacerbated Illness. J Vis Exp.
1119 Levy, Y., Thiebaut, R., Montes, M., Lacabaratz, C., Sloan, L., King, B., Perusat, S., Harrod, C.,
1120 Cobb, A., Roberts, L.K.*, et al.* (2014). Dendritic cell-based therapeutic vaccine elicits
1121 polyfunctional HIV-specific T-cell immunity associated with control of viral load. Eur J Immunol
1122 *44*, 2802-2810.
1123 Lewkowicz, N., Klink, M., Mycko, M.P., and Lewkowicz, P. (2013). Neutrophil--CD4+CD25+ T
1124 regulatory cell interactions: a possible new mechanism of infectious tolerance. Immunobiology
1125 *218*, 455-464.
1126 Li, Y., Wang, W., Yang, F., Xu, Y., Feng, C., and Zhao, Y. (2019). The regulatory roles of
1127 neutrophils in adaptive immunity. Cell Communication and Signaling *17*.
1128 Lim, H.W., Hillsamer, P., Banham, A.H., and Kim, C.H. (2005). Cutting edge: direct suppression
1129 of B cells by CD4+ CD25+ regulatory T cells. Journal of immunology *175*, 4180-4183.
1130 Liu, S., Ren, J., and Ten Dijke, P. (2021). Targeting TGFβ signal transduction for cancer therapy.
1131 Signal Transduction and Targeted Therapy *6*.
1132 Lu, J., Wang, W., Li, P., Wang, X., Gao, C., Zhang, B., Du, X., Liu, Y., Yang, Y., and Qi, F. (2021a).
1133 MiR-146a regulates regulatory T cells to suppress heart transplant rejection in mice. Cell Death
1134 Discov *7*, 165.
1135 Lu, R.J., Taylor, S., Contrepois, K., Kim, M., Bravo, J.I., Ellenberger, M., Sampathkumar, N.K.,
1136 and Benayoun, B.A. (2021b). Multi-omic profiling of primary mouse neutrophils predicts a pattern
1137 of sex and age-related functional regulation. Nat Aging *1*, 715-733.
1138 Lu, Y., and Craft, J. (2021). T Follicular Regulatory Cells: Choreographers of Productive Germinal
1139 Center Responses. Front Immunol *12*, 679909.
1140 Maceiras, A.R., Fonseca, V.R., Agua-Doce, A., and Graca, L. (2017). T follicular regulatory cells
1141 in mice and men. Immunology *152*, 25-35.
1142 Mader, J.S., Ewen, C., Hancock, R.E., and Bleackley, R.C. (2011). The human cathelicidin, LL-
1143 37, induces granzyme-mediated apoptosis in regulatory T cells. J Immunother *34*, 229-235.
1144 Mantovani, A., Cassatella, M.A., Costantini, C., and Jaillon, S. (2011). Neutrophils in the activation
1145 and regulation of innate and adaptive immunity. Nature reviews Immunology *11*, 519-531.

1146 Matsushima, H., Geng, S., Lu, R., Okamoto, T., Yao, Y., Mayuzumi, N., Kotol, P.F., Chojnacki,
1147 B.J., Miyazaki, T., Gallo, R.L.*, et al.* (2013). Neutrophil differentiation into a unique hybrid
1148 population exhibiting dual phenotype and functionality of neutrophils and dendritic cells. Blood
1149 *121*, 1677-1689.
1150 McBride, K.M., Gazumyan, A., Woo, E.M., Schwickert, T.A., Chait, B.T., and Nussenzweig, M.C.
1151 (2008). Regulation of class switch recombination and somatic mutation by AID phosphorylation.
1152 The Journal of experimental medicine *205*, 2585-2594.
1153 Mishalian, I., Bayuh, R., Eruslanov, E., Michaeli, J., Levy, L., Zolotarov, L., Singhal, S., Albelda,
1154 S.M., Granot, Z., and Fridlender, Z.G. (2014). Neutrophils recruit regulatory T-cells into tumors
1155 via secretion of CCL17--a new mechanism of impaired antitumor immunity. Int J Cancer *135*,
1156 1178-1186.
1157 Moore, A.C., Gallimore, A., Draper, S.J., Watkins, K.R., Gilbert, S.C., and Hill, A.V. (2005). Anti-
1158 CD25 antibody enhancement of vaccine-induced immunogenicity: increased durable cellular
1159 immunity with reduced immunodominance. Journal of immunology *175*, 7264-7273.
1160 Morel, C., Badell, E., Abadie, V., Robledo, M., Setterblad, N., Gluckman, J.C., Gicquel, B.,
1161 Boudaly, S., and Winter, N. (2008). Mycobacterium bovis BCG-infected neutrophils and dendritic
1162 cells cooperate to induce specific T cell responses in humans and mice. Eur J Immunol *38*, 437-
1163 447.
1164 Murphy, K.M., Weaver, C., Mowat, A., Berg, L., Chaplin, D., Janeway, C.A., Travers, P., and
1165 Walport, M. (2017). Janeway's immunobiology.
1166 Musich, T., Rahman, M.A., Mohanram, V., Miller-Novak, L., Demberg, T., Venzon, D.J., Felber,
1167 B.K., Franchini, G., Pavlakis, G.N., and Robert-Guroff, M. (2018). Neutrophil Vaccination
1168 Dynamics and Their Capacity To Mediate B Cell Help in Rhesus Macaques. Journal of
1169 immunology *201*, 2287-2302.
1170 Nadkarni, S., Smith, J., Sferruzzi-Perri, A.N., Ledwozyw, A., Kishore, M., Haas, R., Mauro, C.,
1171 Williams, D.J., Farsky, S.H., Marelli-Berg, F.M.*, et al.* (2016). Neutrophils induce proangiogenic T
1172 cells with a regulatory phenotype in pregnancy. Proc Natl Acad Sci U S A *113*, E8415-E8424.
1173 Nauseef, W.M. (2023). Human neutrophils ≠ murine neutrophils: Does it matter? Immunol Rev
1174 *314*, 442-456.
1175 Ndure, J., and Flanagan, K.L. (2014). Targeting regulatory T cells to improve vaccine
1176 immunogenicity in early life. Front Microbiol *5*, 477.
1177 Ohkura, N., Hamaguchi, M., and Sakaguchi, S. (2011). FOXP3+ regulatory T cells: control of
1178 FOXP3 expression by pharmacological agents. Trends Pharmacol Sci *32*, 158-166.
1179 Ono, M. (2020). Control of regulatory T-cell differentiation and function by T-cell receptor
1180 signalling and Foxp3 transcription factor complexes. Immunology *160*, 24-37.
1181 Park, S.R. (2012). Activation-induced Cytidine Deaminase in B Cell Immunity and Cancers.
1182 Immune Netw *12*, 230-239.
1183 Pere, H., Tanchot, C., Bayry, J., Terme, M., Taieb, J., Badoual, C., Adotevi, O., Merillon, N.,
1184 Marcheteau, E., Quillien, V.R.*, et al.* (2012). Comprehensive analysis of current approaches to
1185 inhibit regulatory T cells in cancer. Oncoimmunology *1*, 326-333.
1186 Perobelli, S.M., Mercadante, A.C., Galvani, R.G., Goncalves-Silva, T., Alves, A.P., Pereira-
1187 Neves, A., Benchimol, M., Nobrega, A., and Bonomo, A. (2016). G-CSF-Induced Suppressor IL-
1188 10+ Neutrophils Promote Regulatory T Cells That Inhibit Graft-Versus-Host Disease in a Long-
1189 Lasting and Specific Way. Journal of immunology *197*, 3725-3734.
1190 Pillay, J., Kamp, V.M., Van Hoffen, E., Visser, T., Tak, T., Lammers, J.-W., Ulfman, L.H., Leenen,
1191 L.P., Pickkers, P., and Koenderman, L. (2012). A subset of neutrophils in human systemic
1192 inflammation inhibits T cell responses through Mac-1. Journal of Clinical Investigation *122*, 327-
1193 336.
1194 Pollard, A.J., and Bijker, E.M. (2021). A guide to vaccinology: from basic principles to new
1195 developments. Nature Reviews Immunology *21*, 83-100.

1196 Pollard, A.J., Perrett, K.P., and Beverley, P.C. (2009). Maintaining protection against invasive
1197 bacteria with protein–polysaccharide conjugate vaccines. Nature Reviews Immunology *9*, 213-
1198 220.
1199 Puga, I., Cols, M., Barra, C.M., He, B., Cassis, L., Gentile, M., Comerma, L., Chorny, A., Shan,
1200 M., Xu, W.*, et al.* (2011). B cell-helper neutrophils stimulate the diversification and production of
1201 immunoglobulin in the marginal zone of the spleen. Nature immunology *13*, 170-180.
1202 Qi, J., Liu, C., Bai, Z., Li, X., and Yao, G. (2023). T follicular helper cells and T follicular regulatory
1203 cells in autoimmune diseases. Front Immunol *14*, 1178792.
1204 Rappuoli, R. (2018). Glycoconjugate vaccines: Principles and mechanisms. Sci Transl Med *10*.
1205 Rappuoli, R., De Gregorio, E., and Costantino, P. (2019a). On the mechanisms of conjugate
1206 vaccines. Proceedings of the National Academy of Sciences *116*, 14-16.
1207 Rappuoli, R., De Gregorio, E., and Costantino, P. (2019b). On the mechanisms of conjugate
1208 vaccines. Proc Natl Acad Sci U S A *116*, 14-16.
1209 Raynor, J., Lages, C.S., Shehata, H., Hildeman, D.A., and Chougnet, C.A. (2012). Homeostasis
1210 and function of regulatory T cells in aging. Curr Opin Immunol *24*, 482-487.
1211 Richards, H., Williams, A., Jones, E., Hindley, J., Godkin, A., Simon, A.K., and Gallimore, A.
1212 (2010). Novel role of regulatory T cells in limiting early neutrophil responses in skin. Immunology
1213 *131*, 583-592.
1214 Robinson, G.A., Peng, J., Peckham, H., Butler, G., Pineda-Torra, I., Ciurtin, C., and Jury, E.C.
1215 (2022). Investigating sex differences in T regulatory cells from cisgender and transgender healthy
1216 individuals and patients with autoimmune inflammatory disease: a cross-sectional study. Lancet
1217 Rheumatol *4*, e710-e724.
1218 Sage, P.T., Ron-Harel, N., Juneja, V.R., Sen, D.R., Maleri, S., Sungnak, W., Kuchroo, V.K.,
1219 Haining, W.N., Chevrier, N., Haigis, M.*, et al.* (2016). Suppression by T(FR) cells leads to durable
1220 and selective inhibition of B cell effector function. Nature immunology *17*, 1436-1446.
1221 Schmielau, J., and Finn, O.J. (2001). Activated granulocytes and granulocyte-derived hydrogen
1222 peroxide are the underlying mechanism of suppression of t-cell function in advanced cancer
1223 patients. Cancer research *61*, 4756-4760.
1224 Shafqat, A., Khan, J.A., Alkachem, A.Y., Sabur, H., Alkattan, K., Yaqinuddin, A., and Sing, G.K.
1225 (2023). How Neutrophils Shape the Immune Response: Reassessing Their Multifaceted Role in
1226 Health and Disease. Int J Mol Sci *24*.
1227 Shainheit, M.G., Mule, M., and Camilli, A. (2014). The core promoter of the capsule operon of
1228 Streptococcus pneumoniae is necessary for colonization and invasive disease. Infect Immun *82*,
1229 694-705.
1230 Shevyrev, D., and Tereshchenko, V. (2019). Treg Heterogeneity, Function, and Homeostasis.
1231 Front Immunol *10*, 3100.
1232 Simmons, S.R., Bhalla, M., Herring, S.E., Tchalla, E.Y.I., and Bou Ghanem, E.N. (2021). Older
1233 but not wiser: The age-driven changes in neutrophil responses during pulmonary infections. Infect
1234 Immun.
1235 Soneji, S., and Metlay, J. (2011). Mortality reductions for older adults differ by race/ethnicity and
1236 gender since the introduction of adult and pediatric pneumococcal vaccines. Public Health Rep
1237 *126*, 259-269.
1238 Spitzer, J.A. (1999). Gender differences in some host defense mechanisms. Lupus *8*, 380-383.
1239 Stavnezer, J., Guikema, J.E., and Schrader, C.E. (2008). Mechanism and regulation of class
1240 switch recombination. Annual review of immunology *26*, 261-292.
1241 Stepkowski, S., Bekbolsynov, D., Oenick, J., Brar, S., Mierzejewska, B., Rees, M.A., and
1242 Ekwenna, O. (2024). The Major Role of T Regulatory Cells in the Efficiency of Vaccination in
1243 General and Immunocompromised Populations: A Review. Vaccines (Basel) *12*.
1244 Sterrett, S., Peng, B.J., Burton, R.L., LaFon, D.C., Westfall, A.O., Singh, S., Pride, M., Anderson,
1245 A.S., Ippolito, G.C., Schroeder, H.W., Jr.*, et al.* (2020). Peripheral CD4 T follicular cells induced

1246 by a conjugated pneumococcal vaccine correlate with enhanced opsonophagocytic antibody
1247 responses in younger individuals. Vaccine.
1248 Stream, A., Corriden, R., Dohrmann, S., Gallo, R.L., Nizet, V., and Anderson, E.L. (2024). The
1249 Effect of Retinoic Acid on Neutrophil Innate Immune Interactions With Cutaneous Bacterial
1250 Pathogens. Infect Microbes Dis *6*, 65-73.
1251 Tan, D., Yin, W., Guan, F., Zeng, W., Lee, P., Candotti, F., James, L.K., Saraiva Camara, N.O.,
1252 Haeryfar, S.M.M., Chen, Y.*, et al.* (2022). B cell-T cell interplay in immune regulation: A focus on
1253 follicular regulatory T and regulatory B cell functions. Front Cell Dev Biol *10*, 991840.
1254 Tchalla, E.Y.I., Betadpur, A., Khalil, A.Y., Bhalla, M., and Bou Ghanem, E.N. (2024). Sex-based
1255 difference in immune responses and efficacy of the pneumococcal conjugate vaccine. J Leukoc
1256 Biol.
1257 Tchalla, E.Y.I., Bhalla, M., Wohlfert, E.A., and Bou Ghanem, E.N. (2020). Neutrophils Are
1258 Required During Immunization With the Pneumococcal Conjugate Vaccine for Protective
1259 Antibody Responses and Host Defense Against Infection. J Infect Dis *222*, 1363-1370.
1260 Togashi, Y., Shitara, K., and Nishikawa, H. (2019). Regulatory T cells in cancer
1261 immunosuppression - implications for anticancer therapy. Nat Rev Clin Oncol *16*, 356-371.
1262 Toka, F.N., Suvas, S., and Rouse, B.T. (2004). CD4+ CD25+ T cells regulate vaccine-generated
1263 primary and memory CD8+ T-cell responses against herpes simplex virus type 1. J Virol *78*,
1264 13082-13089.
1265 Trentini, M.M., de Oliveira, F.M., Kipnis, A., and Junqueira-Kipnis, A.P. (2016). The Role of
1266 Neutrophils in the Induction of Specific Th1 and Th17 during Vaccination against Tuberculosis.
1267 Front Microbiol *7*, 898.
1268 Van Gassen, S., Callebaut, B., Van Helden, M.J., Lambrecht, B.N., Demeester, P., Dhaene, T.,
1269 and Saeys, Y. (2015). FlowSOM: Using self-organizing maps for visualization and interpretation
1270 of cytometry data. Cytometry Part A *87*, 636-645.
1271 Vazquez, M.I., Catalan-Dibene, J., and Zlotnik, A. (2015). B cells responses and cytokine
1272 production are regulated by their immune microenvironment. Cytokine *74*, 318-326.
1273 Vidarsson, G., Dekkers, G., and Rispens, T. (2014). IgG Subclasses and Allotypes: From
1274 Structure to Effector Functions. Frontiers in Immunology *5*.
1275 Vinuesa, C.G., Linterman, M.A., Yu, D., and MacLennan, I.C. (2016). Follicular Helper T Cells.
1276 Annual review of immunology *34*, 335-368.
1277 Vono, M., Lin, A., Norrby-Teglund, A., Koup, R.A., Liang, F., and Lore, K. (2017). Neutrophils
1278 acquire the capacity for antigen presentation to memory CD4(+) T cells in vitro and ex vivo. Blood
1279 *129*, 1991-2001.
1280 Wagenvoort, G.H., Sanders, E.A., Vlaminckx, B.J., de Melker, H.E., van der Ende, A., and Knol,
1281 M.J. (2017). Sex differences in invasive pneumococcal disease and the impact of pneumococcal
1282 conjugate vaccination in the Netherlands, 2004 to 2015. Euro Surveill *22*.
1283 Wang, P., and Zheng, S.G. (2013). Regulatory T cells and B cells: implication on autoimmune
1284 diseases. Int J Clin Exp Pathol *6*, 2668-2674.
1285 Weingartner, E., and Golding, A. (2017). Direct control of B cells by Tregs: An opportunity for
1286 long-term modulation of the humoral response. Cell Immunol *318*, 8-16.
1287 Wiemken, T.L., Carrico, R.M., Klein, S.L., Jonsson, C.B., Peyrani, P., Kelley, R.R., Aliberti, S.,
1288 Blasi, F., Fernandez-Gonzalez, R., Lopardo, G.*, et al.* (2014). The effectiveness of the
1289 polysaccharide pneumococcal vaccine for the prevention of hospitalizations due to Streptococcus
1290 pneumoniae community-acquired pneumonia in the elderly differs between the sexes: results
1291 from the Community-Acquired Pneumonia Organization (CAPO) international cohort study.
1292 Vaccine *32*, 2198-2203.
1293 Wiese, A.D., Grijalva, C.G., Zhu, Y., Mitchel, E.F., Jr., and Griffin, M.R. (2016). Changes in
1294 Childhood Pneumonia Hospitalizations by Race and Sex Associated with Pneumococcal
1295 Conjugate Vaccines. Emerg Infect Dis *22*.

1296 Xie, M.M., Chen, Q., Liu, H., Yang, K., Koh, B., Wu, H., Maleki, S.J., Hurlburt, B.K., Cook-Mills,
1297 J., Kaplan, M.H.*, et al.* (2020). T follicular regulatory cells and IL-10 promote food antigen-specific
1298 IgE. J Clin Invest *130*, 3820-3832.
1299 Yang, P., Li, Y., Xie, Y., and Liu, Y. (2019). Different Faces for Different Places: Heterogeneity of
1300 Neutrophil Phenotype and Function. J Immunol Res *2019*, 8016254.
1301